Dissertation Thesis for Integrated Master in Mechanical Engineering

Characterization of the fatigue behavior of a structural adhesive for high performance applications

by

João Paulo Ferreira Monteiro

Supervisor:

Lucas Filipe Martins da Silva

Co-supervisors:

Alireza Akhavan
Ricardo Carbas
Eduardo Marques

Porto, February 2019

Abstract

The use of adhesives as a structural bonding component has been increasing globally, mostly because of the advantages related to performance and cost over the conventional bonding methods.

With the increased use of adhesives in industries, it becomes important to characterize the adhesive under conditions similar to the real working conditions. Fracture mechanics tests provide important tools to evaluate adhesive joints strength. The joints experience mixed mode and mostly cyclic stresses conditions during their service life.

The aim of this dissertation is to study the fatigue and fracture behavior of an adhesive, considering pure and mixed mode loadings. Double Cantilever Beam (DCB) and End-Notched Flexure (ENF) tests were performed to determine mode I and mode II fracture and fatigue behavior. For testing under mixed mode conditions, an apparatus was used to obtain the fracture and fatigue behavior. The energy release rate was calculated by considering an equivalent crack length method, called the Compliance Based Beam Method (CBBM). A data degradation approach for pure mode II fatigue loading conditions was also developed, using an Abacus user element subroutine. Finally, a study was performed on the effects of load level and load ratio on the mode I fatigue crack growth behavior and Paris law parameters.

Resumo

A utilização de adesivos estruturais tem aumentado globalmente, principalmente devido às vantagens relacionadas com o desempenho e custo em relação aos métodos convencionais de ligação.

Com o aumento do uso de adesivos nas indústrias, torna-se importante caracterizar o adesivo sob condições semelhantes às condições reais. Os testes de normalizados da mecânica fratura fornecem ferramentas importantes para avaliar o comportamento de juntas adesivas. No entanto, em situações reais, as juntas experienciam solicitações de modo misto e na maioria das vezes cargas cíclicas durante a sua vida de serviço.

O objetivo desta dissertação é estudar o comportamento à fadiga e fratura de um adesivo, quando sujeito a solicitações em modo puro e modo misto. Para determinar o comportamento à fadiga e fratura em modo I e em modo II, efetuaram-se os ensaios Double Cantilever Beam (DCB) e End Notched Flexure (ENF), respetivamente. Relativamente ao estudo de modo misto, foi utilizado um dispositivo que permite o estudo de várias combinações de carga entre modo I e modo II. A taxa de libertação de energia foi calculada recorrendo a um método baseado no conceito de fenda equivalente, Compliance Based Beam Method (CBBM). Foi também desenvolvido um modelo numérico de degradação para condições de fadiga para puro modo II usando uma sub-rotina do ABAQUS. Ao realizar testes de fadiga para modo I com diferentes percentagens da carga quase-estática máxima, foi possível determinar o efeito do nível e da razão de carga no crescimento da fenda.

Acknowledgments

I would like to express my gratitude to Prof. Lucas da Silva for the advices and for sharing his vast knowledge.

I would like to thank my co-supervisors Alireza Akhavan, Ricardo Carbas and Eduardo Marques for the continuous guidance and for the lessons

I am grateful for being a part of ADFeup group, and I would like to thank every member of the group.

And finally, I want to express thanks my family, my girlfriend and friends for all the support.

Contents

1. Introduction

1.1. Background and motivation

During the past decades, the use of adhesives as a structural bonding component has been increasing in a wide range of industries such as automotive, aerospace, aeronautical, among others.[1]. Several studies have been published, showing the inherent advantages of adhesive joints over the conventional mechanical joining methods [2] [3]. The use of adhesive as a structural bonding component offers a more uniform stress distribution over the bonded area, avoiding stress concentrations, reduced weight, ability to bond dissimilar materials and confers some flexibility to the joint, increasing the resistance to dynamic loads [1]. Within this context, to design durable joints it is crucial to fully understand the mechanical behavior of the adhesive and the joint. Due to that, experimental methods must be developed to obtain and predict the joint behavior on static and fatigue conditions [4].

Fracture mechanics tests offers important tools to calculate adhesive joint strength [5]. However, in real applications, the joints will be under mixed mode stresses, and it is important to determine the fracture energy for pure mode I [6], pure mode II [7] and mixed mode [8] [9]. To do so, Double Cantilever Beam (DCB) tests for pure mode I [10], and End Notched Flexure (ENF) tests for pure mode II were performed. To obtain the fracture energy for mixed mode, an apparatus was used to test the joints. The critical energy release rate for pure modes and the energy release rate for mixed mode were obtained using a Compliance Based Beam Method (CBBM) which determines an equivalent crack length using the information from the experimental tests. With the energy values for different modes it was possible to determine the fracture envelope of the adhesive, which can provide important information in order to predict the fracture energy for every possible mixed mode.

Many of the adhesive joint failures are caused by fatigue degradation. This degradation is defined as a loss of properties over time due to alternating stresses. The fatigue behavior of an adhesive can be evaluated through the measurement of the fatigue crack growth (FCG) and the Paris law parameters in joints subjected to the same loading conditions. With the slope of the Paris law curve, for different mode mixities, the slope envelope can be determined. The study of the effect of the loading conditions is also a very important task, as in real joints, there are infinity combinations of loading conditions (percentage of quasi-static load and load ratio).

1.2. Problem definition

The main problem that this thesis attempts to address is the lack of material data and numerical procedures available for the prediction of the fatigue life of adhesive joints. As previously stated, as industrial users increasingly adopt adhesive joints so does increase to necessity of having accurate tools for predicting the joint behavior and ensuring that they have the necessary durability for the intended applications.

1.3. Objectives

The aim of this study is to investigate the fatigue fracture behavior of an epoxy adhesive using the Paris law and by employing the CBBM approach. By measuring the minimum fracture energy for each loading cycle, the effects of the loading conditions on the ratio of G_{min}/G_{max} were also studied. Another main objective of this work was to extend an already existing mode I data degradation approach for pure mode II. For this purpose, a triangular shape cohesive zone model in combination with a data degradation method were considered in the development of an Abaqus user element (UEL) subroutine.

1.4. Research methodology

The methodology adopted for this thesis consisted on the experimental testing of several specimens to determine the fatigue behavior under pure mode I, pure mode II and mixed

mode loading. This experimental data was then used to construct numerical models able to degrade the adhesive properties under cyclic loadings.

1.5. Outline of the thesis

This thesis is presented as two separate research papers. The objective of the work described in Paper 1 was to develop a data degradation approach for pure mode II fatigue loading conditions. An Abaqus user element subroutine was developed for degrading the cohesive properties of the elements based on the extended data degradation approach and the triangular cohesive zone model (CZM).

The aim of Paper 2 was to obtain the fracture energies, which enables the construction of the fracture envelope, and the characterization the fatigue behavior, through the analysis of the Paris law parameters. Such approach makes it possible to evaluate the influence of the loading conditions on the fatigue crack growth.

2. Experimental procedures

2.1. Materials

An epoxy-based adhesive was considered to bond metallic substrates. The mechanical properties of the adhesive were determined through bulk specimens and thick adherend shear tests (TAST) and are listed in Table 1.

The substrates were machined from DIN 40CrMnMo7 steel (high strength steel to avoid plastic deformation), with the mechanical properties also being given in Table 1.

Table 1 - Mechanical properties of the adhesive and the substrate

Properties	Substrate	Adhesive
Tensile strength (MPa)	-	31.3±0.6
Tensile strain to failure (%)	-	10.4±0.5
Shear strength (MPa)	-	23.1±0.5
Shear strain to failure (%)	-	43.3±0.9
Young's modulus (MPa)	210000	1159±29.3
Shear modulus (MPa)	-	440±8.7
Poisson's ratio (ν)	0.3	
Mode I fracture energy (N/mm)	-	2.2
Mode II fracture energy (N/mm)	-	14.4

2.2. Test methods

Bulk, TAST, DCB, ENF and mixed mode (at 45º) tests were performed under quasi static condition at room temperature with a displacement rate of 0.2 mm/min. CBBM data reduction was implemented for data treatment of the fracture mechanics tests (DCB, ENF and mixed mode), allowing increased accuracy of the fracture energy measurements. Quasi-static testing was followed by a fatigue testing procedure with the purpose of assessing the relevant material data under cyclic loads. Table 2 displays the different conditions used for the fatigue tests for mode I, mode II and mixed mode.

Table 2 - load conditions used in fatigue tests

	Number of specimens	Load level of quasi-static load	Load ratio
Mode I	5	60%	10% and 30%
	2	40%	10% and 30%
	1	35%	30%
		30%	
Mode II	5	60%	10%
Mixed mode	5		

Bulk specimen tensile testing

Bulk tests use a specimen with a specific shape (Figure 1), obtained from a cured sheet of adhesive, and are tested under tensile loads. The load and displacement is registered and used to create a stress-strain curve. From this curve, the elastic modulus, tensile strength can be extracted, and the ductility can be assessed.

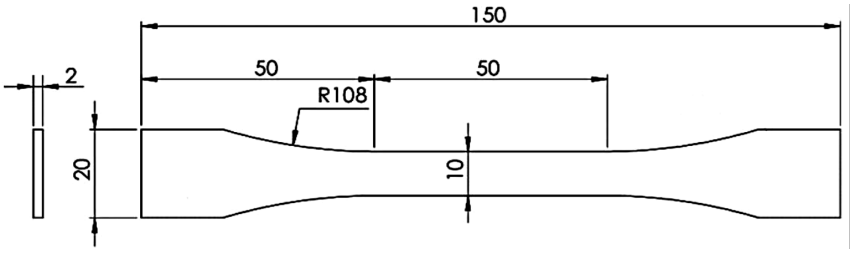

Figure 1 - Bulk specimen geometry (dimensions in mm)

Thick adherend shear test (TAST)

To obtain the shear strength properties of the adhesive TAST specimens were manufactured and tested. The TAST specimens were tested at quasi-static loading rates, with the load and extension being registered during the test. The extension in the adhesive layer is measured using a clip gage type of extensometer. Figure 2 shows the geometry of a TAST specimen.

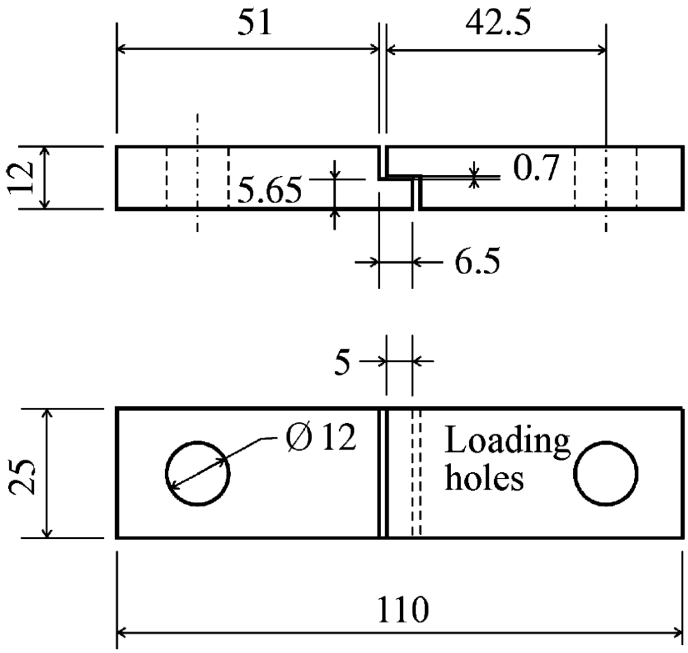

Figure 2 - TAST specimen geometry (dimensions in mm)

Double cantilever beam (DCB)

The most commonly used test to characterize the mode I fracture behavior of adhesives is the DCB test. This test applies a peel load to an adhesive layer located between two thick substrates, inducing crack propagation. A schematic of the test set up is shown in Figure 3.

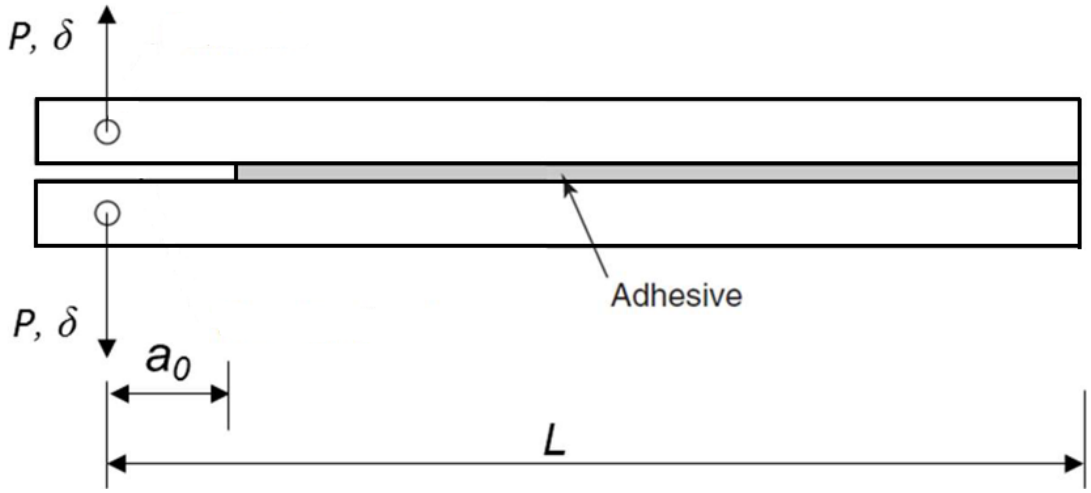

Figure 3 - Schematic representation of the DCB test [4]

The specimens were manufactured with a bondline thickness of 0.3 mm, achieved using calibrated metal spacers. To guarantee a consistent pre-crack size (45 mm) of the specimens, a thin blade was placed on one edge of the in the adhesive layer. Before actual testing is performed, the specimens must be subjected to a pre-cracking procedure, where the specimen is slowly loaded until the onset of crack propagation is detected. When this occurs, the pre-cracking procedure is immediately stopped, the blade is removed, and the resulting pre-crack length is measured and registered.

End Notched Flexure (ENF)

According to de Moura et al. [7], the ENF is considered to be most appropriate test procedure for fracture characterization in mode II. A schematic drawing of the tested specimen is shown in Figure 4.

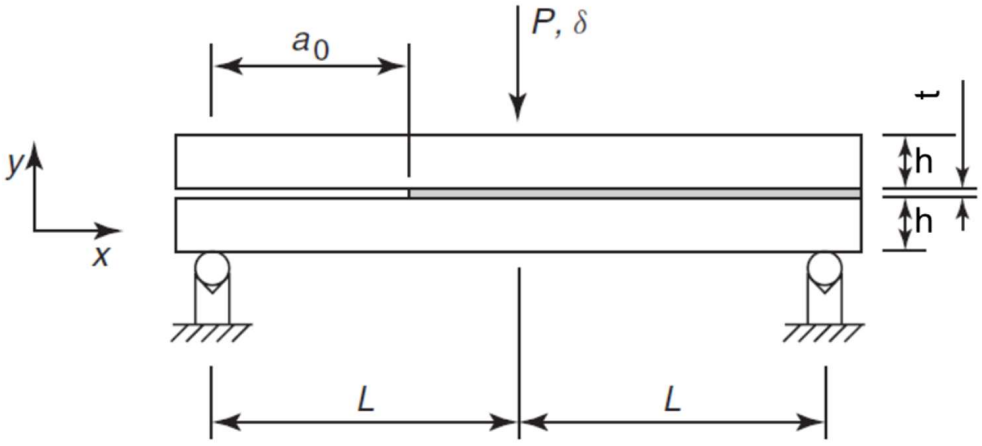

Figure 4 - Schematic representation of the ENF test [4]

The specimen geometry for the ENF is exactly the same as that used for the DCB test, only the loading conditions are changed. This is an extremely practical consideration for this type of research work as the manufacture process of the specimens can be performed simultaneously.

Mixed mode testing

To overcome the existing difficulties of measuring mixed mode fracture toughness, a mixed mode testing apparatus was developed by the *ADFeup* group [11] specifically suited for testing the fracture behavior of structural adhesives. The apparatus uses the same specimens as the DCB and the ENF, again greatly simplifying the manufacture process, as a single specimen geometry can be used to assess the behavior of the adhesive under any type of loading condition. The geometry of the apparatus is presented in Figure 5.

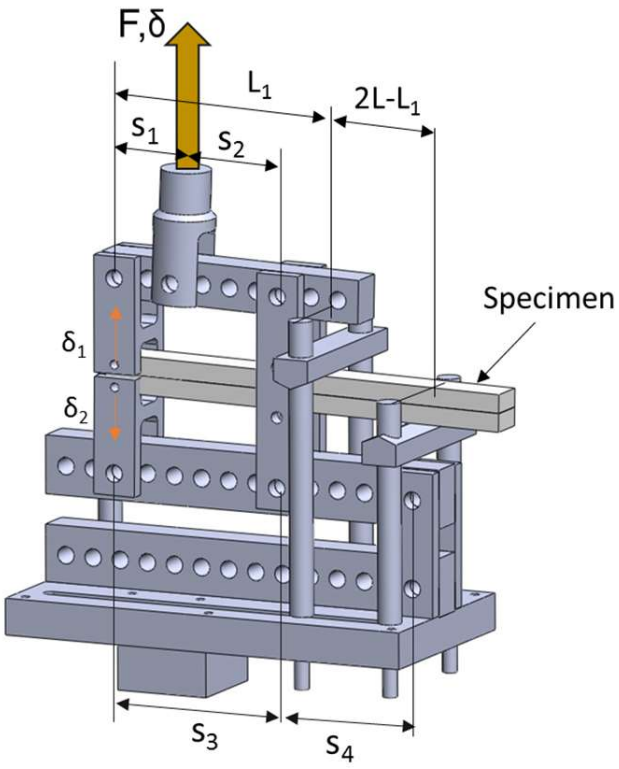

Figure 5 - scheme of the mixed mode apparatus used [11]

By changing the beam lengths (s_1,s_2, s_3 and s_4) the apparatus can be configured for multiple phase angles between pure mode I and II. This phase angle and the forces applied to the top and bottom arms of the specimens change according to the beam lengths. The angle (as a function of the upper beam load - F_1 and the lower beam load - F_2) is given by:

$$\varphi_{apparatus} = \tan^{-1} \frac{\sqrt{3}\left(\frac{F_1}{F_2} + 1\right)}{2\left(\frac{F_1}{F_2} - 1\right)} \quad (1)$$

The load applied through the apparatus is therefore a combination of mode I and mode II. Figure 6 shows how the apparatus setup can be decomposed into two separate mode I (DCB) and mode II (ENF) components.

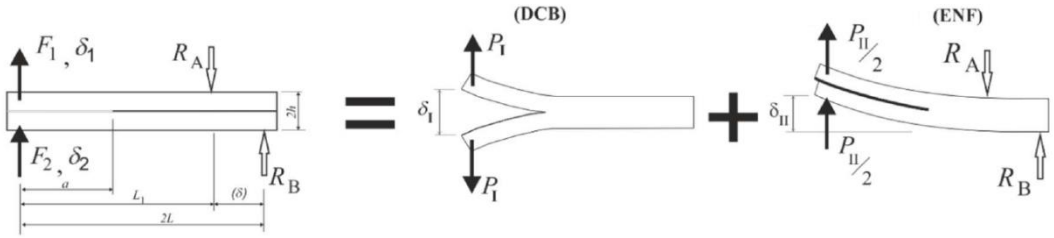

Figure 6 Schematic representation of the specimen loading with mode I and mode II partition [5]

The load applied by the machine is decomposed in two distinct loads, corresponding to the top and bottom loads, F_1 and F_2 respectively (see Figure10). The relation is given by:

$$F_1 = F\frac{s_1}{s_3};\ F_2 = F\frac{s_1 s_4}{s_3(s_3 + s_4)} \quad (2)$$

Mode I and mode II load components, P_I and P_{II} are determined by:

$$P_I = \frac{F_1 - F_2}{2};\ P_{II} = F_1 + F_2 \quad (3)$$

3. Numerical modelling

An Abaqus user element subroutine was developed for degrading the cohesive properties of the elements based on the extended data degradation approach. To achieve this, finite element method (FEM) was employed in combination with the triangular cohesive zone CZM (Figure 7).

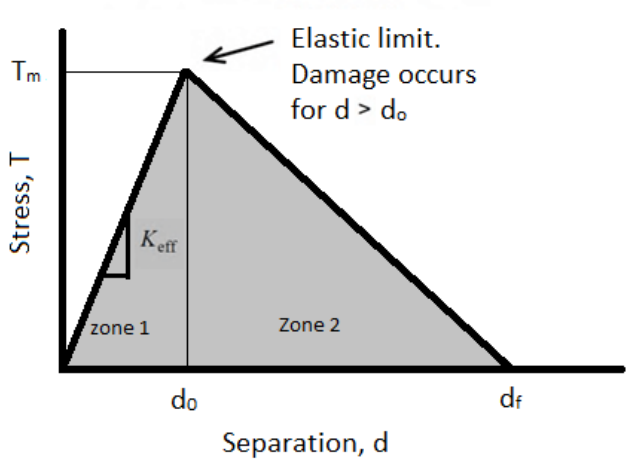

Figure 7 - Triangular Abaqus traction-separation law

Figure 7 shows a triangular shaped traction separation law where the d_0 and d_f correspond, respectively, to the displacement at which the damage initiates and at the final failure of the element. K_{eff} is the effective initial stiffness. The triangle is limited by the yield stress of the material (T_m), which occurs at the d_0 displacement. A schematic view of a cohesive zone model applied to an ENF specimen is shown in Figure 8. The customized element should be defined for the adhesive layer. Using Abaqus/CAE, the static load based on the maximum load of fatigue test, should be applied to the middle of the specimen, which results in separation of the nodes over the cohesive element based on the degradation of the element properties, which eventually leads to crack propagation. The cohesive properties of the adhesive layer are defined by modifying the input file. The basics of the FEM, shape functions, the shape of the CZM and the cycle by cycle degradation of the cohesive properties of the element are defined by the creation of a Fortran user element subroutine (UEL) code implemented in Abaqus.

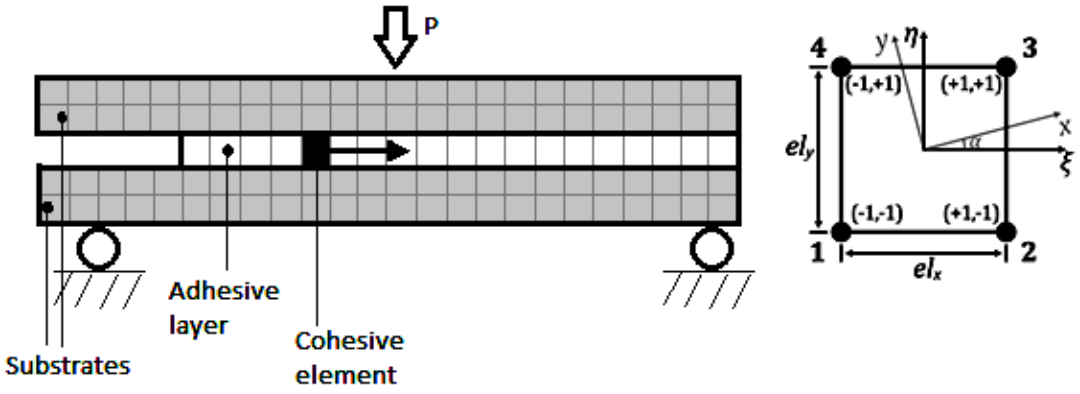

Figure 8 – Schematic of the ENF specimen and the cohesive zone element in global (x,y) and local (ξ,η) coordinates

The degradation models are basically semi-empirical relations which are based on the experimental results where the value of the failure parameter is a function of the number of fatigue cycles. Recently, a degradation model for mode I fatigue life estimation of adhesive material was proposed by Costa et al. [12] as follows:

$$y(N) = y_0 \left(1 - \frac{N}{N_f}\right)^k \tag{14}$$

where N and N_f are the numbers of cycles being evaluated and the cycles at failure respectively. The superscript k is the coefficient of the degradation rate which is obtained by fitting the experimental data with the numerical results. y and y_0 correspond to the property of the cohesive zone law being degraded and the initial value of that property without any degradation before the cyclic test. N_f should be already known based on the proposed method.

4. Conclusions

The static and fatigue behavior of a structural epoxy-based adhesive was studied under pure and mixed loading modes. Based on the static results, the fracture envelope of the adhesive was experimentally obtained, and the envelope of the Paris law slope (m) was obtained as a function of different mode mixities. Different loading conditions were considered to study the effects of load level and R ratio on the fatigue behavior of the adhesive. It was observed that the use of higher loads (amplitude) leads to a faster crack propagation and consequently a shorter life. Result showed that the effect of load level on fatigue crack propagation is more pronounced for lower R-ratios. It was also found that the threshold fracture energy (G_{th}) can be considered as constant for different mode I loading conditions. However, it was also observed that G_{th} is a function of the mode mixity.

A UEL subroutine was prepared and implemented into Abaqus to analyse the degradation of the cohesive properties of the elements based on the degradation model. The damage initiation and damage evolution were calculated based on a triangular shaped CZM.

Fatigue tests were also performed on end notched flexure (ENF) specimens to calibrate the degradation model. By adjusting the calibration parameter and fitting the experimental data with the numerical results, it was found that the degradation approach can be applied for pure mode II loading conditions. As the adhesive joints are mostly designed for shear loading conditions (instead of peel stress), the introduced approach can be considered as a useful tool for fatigue life estimation of adhesive joints.

5. Future works

The study of the fracture behavior of adhesives under fatigue conditions is still a relatively unexplored, and several interesting studies can be suggested in this field, especially be considering environmental conditions. For example, the fracture and fatigue behavior of the adhesive under different testing temperatures is a very relevant subject as many adhesive joints in advanced structures are expected to operate cyclically at temperatures above the room temperature. Similarly, the combined effect of fatigue and ageing is also very relevant for real world applications, as adhesives will present significantly changed properties as they absorb water.

References

1. Da Silva, L.F., A. Öchsner, and R.D. Adams, *Handbook of adhesion technology*. 2011: Springer Science & Business Media.
2. Chowdhury, N., et al., *Static and fatigue testing thin riveted, bonded and hybrid carbon fiber double lap joints used in aircraft structures.* 2015. **121**: p. 315-323.
3. Moroni, F. and A. Pirondi, *Technology of rivet: adhesive joints*, in *Hybrid Adhesive Joints*. 2010, Springer. p. 79-108.
4. Da Silva, L.F., et al., *Testing adhesive joints: best practices*. 2012: John Wiley & Sons.
5. Chaves, F.J., et al., *Fracture mechanics tests in adhesively bonded joints: a literature review.* 2014. **90**(12): p. 955-992.
6. Blackman, B., et al., *Measuring the mode I adhesive fracture energy, GIC, of structural adhesive joints: the results of an international round-robin.* 2003. **23**(4): p. 293-305.
7. De Moura, M., et al., *Pure mode II fracture characterization of composite bonded joints.* 2009. **46**(6): p. 1589-1595.
8. Da Silva, L., V. Esteves, and F.J.M.u.W. Chaves, *Fracture toughness of a structural adhesive under mixed mode loadings.* 2011. **42**(5): p. 460-470.
9. Fernlund, G., J.J.C.s. Spelt, and technology, *Mixed-mode fracture characterization of adhesive joints.* 1994. **50**(4): p. 441-449.
10. ASTM, D.J.A.B.o.A.S., *Standard test method for fracture strength in cleavage of adhesives in bonded metal joints.* 1999. **15**: p. 212-218.
11. Costa, M., et al., *An apparatus for mixed-mode fracture characterization of adhesive joints.* 2017. **91**: p. 94-102.
12. Costa, M., et al., *A cohesive zone element for mode I modelling of adhesives degraded by humidity and fatigue.* International Journal of Fatigue, 2018. **112**: p. 173-182.

Paper 1

Mode II modeling of adhesive materials degraded by fatigue loading using cohesive zone elements

J. Monteiro[1], A. Akhavan-Safar[2], R. Carbas[2], E. Marques[2], R Goyal[3], Mohamed El-zein[4], L.F.M da Silva[1]

[1]Department of Mechanical Engineering, Faculty of Engineering of the University of Porto, Rua Dr. Roberto Frias, 4200-465 Porto, Portugal

[2]Institute of Science and Innovation in Mechanical and Industrial Engineering (INEGI), Rua Dr. Roberto Frias, 4200-465 Porto, Portugal

[3]Deere & Company, Asia Technology and Innovation Center, Pune, MH, India

[4]Deere & Company, MTIC, One John Deere Place, Moline, Il. 61265, United States

Abstract

Because of maintenance issues, the concept of safe life is an important philosophy for designing adhesive joints where the service load is cyclic. However, this philosophy needs a tool to be able to estimate the total fatigue life. The objective of this study is to develop a numerical tool to predict the fatigue life of adhesive joints for pure mode II loading conditions. To achieve this, a previously published mode I data degradation approach was extended for pure mode II. Fatigue tests were performed on end notched flexure (ENF) specimens to calibrate the degradation model. A triangular shape cohesive zone model (CZM) in combination with a data degradation method were considered in an Abaqus user element (UEL) subroutine. Based on the results, it was found that the proposed method can be applied for fatigue life estimation of adhesive joints in pure mode II conditions as well as pure mode I.

Keywords: Adhesive joints, Fatigue life, Pure mode II, User element, Cohesive zone model, Paris law.

1. Introduction

Due to their advantages compared to classical fastening methods, the application of adhesive joints has greatly increased in several advanced industries such as automotive, aeronautical and aerospace [1]. This bonding approach offers a more uniform stress distribution over the bonded area, is able to bond dissimilar materials, reduces weight and increases resistance to dynamic loadings [1]. Due to the growing industrial demand to use adhesive joints for bonding primary structures, numerical tools must be developed and combined with predictive tools of the joint strength as a function of different loading conditions.

In terms of industrial design, safe life can be a good philosophy for designing adhesive joints where almost no maintenance or repair is required during the service life. However, estimation of the total life is the most important point in the safe life design concept. To achieve this, the development of a powerful analytical or numerical tool for fatigue life estimation of adhesive strength is crucial. CZM is a useful approach for modelling composite delamination and is widely applied on adhesive joints as well. The combination of the finite element method (FEM) and CZM concepts creates a useful tool for failure assessment of adhesively bonded joints. The CZM concept was first proposed by Dugdale and Barenblatt [2, 3] and then developed by other authors [4, 5]. To relate the traction to the damage, different CZM shapes have been developed. Triangular [6], trapezoidal [7], exponential [8], and some more complex laws [9, 10] are the most common CZM shapes. Although, the majority of CZM studies regarding adhesively bonded joints is aimed at static applications, several environmental and loading parameters, such as humidity or cyclic loading have also recently been considered for the development of new cohesive zone elements. For modeling the effect of cyclic loads,

some researchers [11-13] have applied a damage evolution using a cycle-by-cycle analysis. Turon et al. [14] used a cycle extrapolation technique. Some authors [15, 16] made the analysis based on the maximum fatigue load. In some studies [11, 17], the damage factor was controlled as a function of the range of applied strain energy release rate. Fatigue behavior of adhesive materials in pure mode II conditions as a challenging loading mode is also considered by some authors [18].

Recently, a fatigue degradation relation was proposed by Costa et al. [19] for pure mode I loading conditions. However, as the adhesive joints in real applications mostly experience shear stresses, in the current work, the mentioned degradation model is developed for pure mode II fatigue loading conditions. ENF fatigue tests were performed to calibrate and evaluate the extended data degradation model. An Abaqus user element subroutine was developed for degrading the cohesive properties of the elements based on the extended data degradation approach and the triangular CZM.

2. Experimental details

In the experimental procedure, ENF specimens were manufactured and tested in static and fatigue loading conditions. The aim of these tests was the determination of both the fracture energy and the Paris law parameters for a pure mode II loading condition.

2.1. Materials

A high performance one-component epoxy-based past with the viscosity of 30-50 Pa.s was used as adhesive. The main application of the adhesive is for metal to metal bonding where high durability and stiffness are required. The mechanical properties of the adhesive were determined through bulk specimens and thick adherend shear tests (TAST) and are listed in Table 1. A typical tensile stress-strain curve of the adhesive is presented in Figure 1, showing significant ductility. The substrates were machined from DIN

40CrMnMo7 steel (high strength steel to avoid plastic deformation), with the mechanical properties also being given in Table 1.

2.2. Joint geometry and preparation

ENF specimen were manufactured with a bondline thickness of 0.3 mm. The substrate geometry used to perform the static and fatigue tests follows ASTM D-3433-99 standard (Figure 2). Before bonding the steel substrates, the surfaces were sandblasted and then degreased with acetone. Calibrated metal spacers were placed at both ends of the joints to guarantee the bond line thickness defined. Using a thin blade at the start of the adhesive layer, a similar pre-crack size (45mm) was introduced to the specimens. The curing process for the adhesive includes three stages, heating ramp, soak time and cooling down, all carried out with a constant pressure of 25 bar. To accomplish this, a hot plate press was utilized in order to control the temperature and pressure of the curing process. The temperature and the curing time were set to 177ºC and 20 min respectively. After curing, the specimens side surfaces were abraded with sandpaper to avoid the influence of the extra adhesive on the test results. All specimens were kept at room conditions for 72h before the test. All specimens were submitted to a pre-cracking procedure to promote stable crack propagation before testing. All blades were removed before the test.

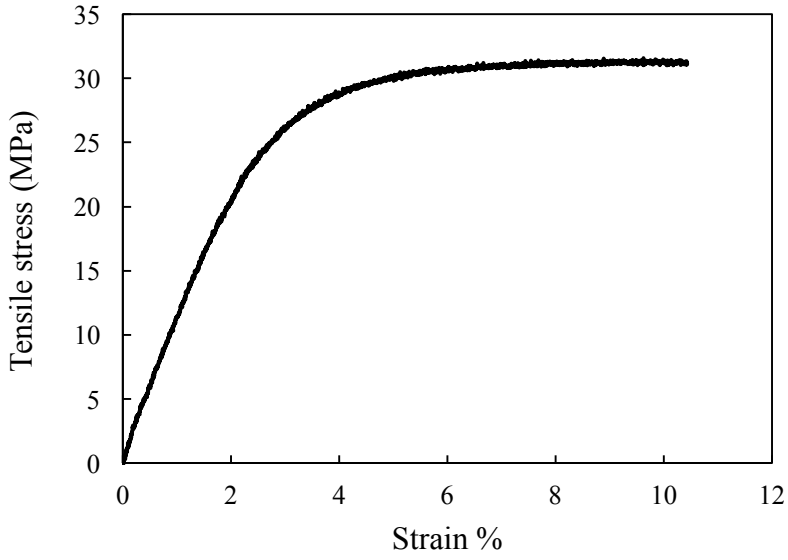

Figure 1 - Typical tensile stress-strain curve

Table 1 - Mechanical properties of the adhesive and the substrate

Properties	Substrate	Adhesive
Tensile strength (MPa)	-	31.3±0.6
Tensile strain to failure (%)	-	10.4±0.5
Shear strength (MPa)	-	23.1±0.5
shear strain to failure (%)	-	43.3±0.9
Young's modulus (MPa)	210000	1159±29.3
Shear modulus (MPa)	-	440±8.7
Poisson's ratio (ν)	0.3	

2.3. Testing conditions

According to da Moura et al. [20], the ENF appears to be the most appropriate test procedure for fracture characterization in mode II. A schematic drawing of the tested specimen is shown in Figure 2 and the test setup is shown in Figure 3.

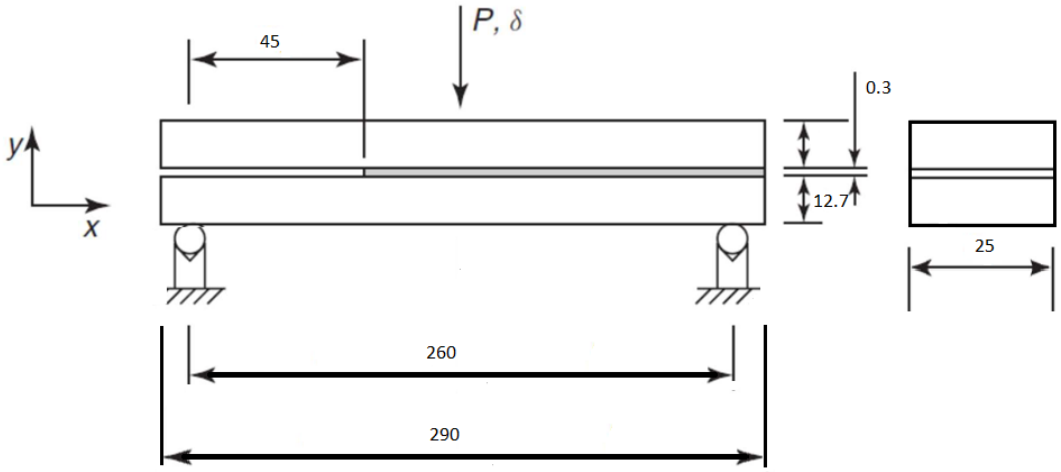

Figure 2 - Specimens geometry according to ASTM D-3433-99 (dimensions in millimeters)-Schematic representations of the ENF test adapted

Figure 9 - Outline of the ENF test setup

To reduce the friction between the adherends as the crack progresses, a Teflon sheet lubricated with oil was placed in the cracked end of the specimen (see Figure 3). The load was applied in the middle of the specimen which corresponds to the middle point of the two supports.

A universal testing machine was used to record the load and displacement data. ENF tests were performed at room temperature and with a displacement rate of 0.2 mm/min for static conditions.

For assessing fatigue behavior, the test was performed at load control conditions with the load level set at 60% of the maximum static strength and the load ratio (the ratio of minimum load to the maximum load) was set to 0.1. The loading frequency was defined as 10Hz. The load and displacement data were recorded for each cycle until the joint failed. 5 specimens were tested for the mentioned loading conditions.

3. Finite element programming

3.1. Finite element method (FEM)

FEM is a useful approach to find an approximate solution of problems with complex geometries or loading conditions. According to the FEM, the structure is discretized into several smaller sub-domains called elements. The concepts of FEM are based on calculating the displacement of the elements as a function of the applied loads and boundary conditions. To achieve this, the stiffness matrix of the element should be defined. The stiffness matrix gives information about the behavior of the elements and indicates the resistance of the element against deformation. Accordingly, to estimate the behavior of the element, FEM solves the following equation:

$$[K]\times\{d\} = \{f\} \quad (1)$$

where $[K]$, $\{d\}$ and $\{f\}$ are the stiffness matrix, the displacement vector which is obtained by FEM and the vector of the external forces, respectively. On the other side, CZM as a fracture mechanics approach, uses the traction separation laws for damage analysis of the materials. In the current work where CZM is considered for damage analysis of the adhesive, the stiffness matrix and the vector of the external forces are obtained using the following matrix formulations:

$$[K] = w[B]^T[T_d][B]$$

$$\{f\} = w[B]^T\{T\} \quad (2)$$

where w and $[B]$ are the element width and the matrix of the global displacement-separation relation. $\{T\}$ and $[T_d]$ are also vector and matrix, respectively and include the traction-separation laws. There are various traction-separation laws, such as, triangular, trapezoidal, exponential, etc. Based on the behavior of the material, the shape of the traction-separation law will change and consequently will lead to different formulations for the $\{T\}$ and $[T_d]$. For the purposes of the present work, the triangular traction-separation shape, the most commonly employed CZM shape, was considered. Figure 4 shows a typical triangular traction-separation shape.

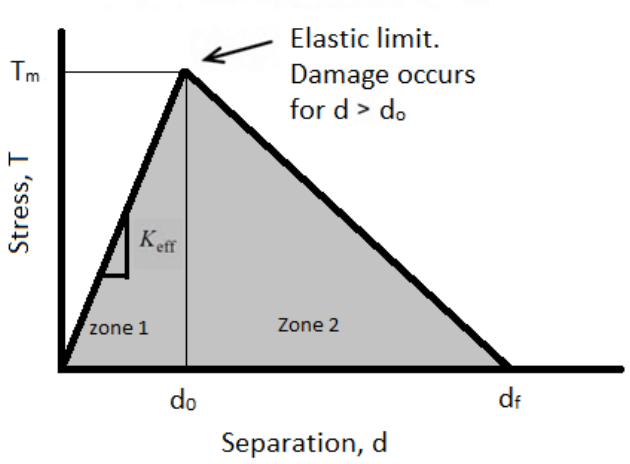

Figure 4 - Triangular Abaqus traction-separation law

For mode II loadings in the local coordinate system (see Figure 5) $\{T\}$ and $[T_d]$ are defined as:

$$\{T\} = \begin{Bmatrix} t(d) \\ 0 \end{Bmatrix} \quad [T_d] = \begin{bmatrix} t'(d) & 0 \\ 0 & 0 \end{bmatrix} \tag{3}$$

where *t(d)* corresponds to the equation that define the triangular shape CZM. d_0 and d_f correspond to the displacement where the damage initiate and the final failure of the element. K_{eff} is also the effective initial stiffness which is defined later in this paper.

3.2. Cohesive element and UEL subroutine

For the developed cohesive element, basic FEM concepts must be first defined, such as number of nodes, shape functions of the elements and matrices introduced earlier. A schematic view of an ENF specimen is shown in Figure 5. The customized element should be defined for the adhesive layer. Using Abaqus/CAE, the static load based on the maximum load of fatigue test, should be applied to the middle of the specimen, which results in separation of the nodes over the cohesive element based on the element property degradations, which finally leads to crack propagation. The cohesive properties of the adhesive layer were defined by modifying the input file. The basics of the FEM, shape functions, the shape of the CZM and the cycle by cycle degradation of the cohesive properties of the element were defined in a Fortran user element subroutine (UEL) code implemented in Abaqus.

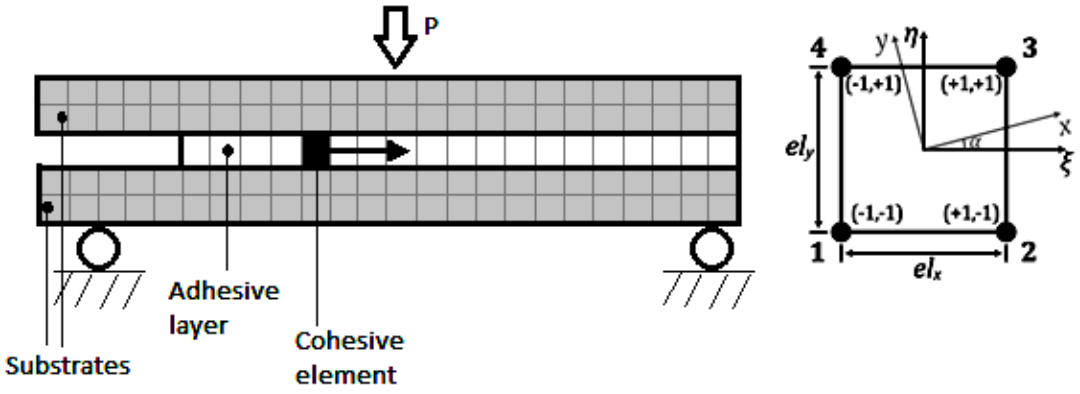

Figure 5 – Schematic of the ENF specimen and the cohesive zone element in global (x,y) and local (ξ,η) coordinates

According to Figure 5, based on the basics of the FEM programming, two different coordinates are defined. One of them is the local coordinate which is a coordinate system of the elements, and the other one is the global coordinate, which is the original coordinate of each node. In this work, a 4-node linear element was employed in the UEL subroutine

where typically 4 shape functions are required to be defined. It is important to mention, that for large models with a high number of total elements, the element may be improved to support additional nodes (6 or 8 nodes). For formulation resolution, the cohesive element may serve as a contact element ($el_y = 0\ mm$, see Figure 5), or as an element with finite height ($el_y > 0\ mm$). In this research, for formulation purposes the height of the cohesive element was considered null ($el_y = 0\ mm$), therefore it is only needed to create form functions for node 1,4 and 2,3. At a specific ξ coordinate, the same functions apply to both nodes:

$$N_{1,4} = \frac{1}{2}(1 - \xi); \quad N_{2,3} = \frac{1}{2}(1 + \xi); \tag{4}$$

From eq. (4), matrix $[N]$ which represents the matrix of the shape functions can now be determined as follows:

$$[N] = \begin{bmatrix} N_{1,4} & & N_{2,3} & & N_{2,3} & & N_{1,4} & \\ & N_{1,4} & & N_{2,3} & & N_{2,3} & & N_{1,4} \end{bmatrix} \tag{5}$$

The strain displacement is represented by matrix $[B]$:

$$[B] = [R][N] \tag{6}$$

Where matrix $[R]$ as the transformations matrix from global to local coordinates is defined as:

$$[R] = \begin{bmatrix} \cos\alpha & \sin\alpha \\ -\sin\alpha & \cos\alpha \end{bmatrix} \tag{7}$$

α is the angle between the coordinate systems (see Figure 5).

3.3. Traction-separation law

$\{T\}$ and $[T_d]$ are functions of the used CZM shape. Based on the considered triangular CZM shape two different zones (zones 1 and 2 shown in Figure 4) can be considered for determining the values of $t_i(d)$, $t_i{}'(d)$ and G_i. If the shear displacement of the element is

less than d_0 the zone number is 1. Therefore, $t_1(d), t_1{}'(d)$ (traction matrix and the derivative of the traction matrix) are defined as follows:

$$t_1(d) = \frac{t_m d}{d_0} \tag{8}$$

$$t_1'(d) = \frac{t_m}{d_0} \tag{9}$$

where the subscripts 1 and 2 denote the zone 1 and zone 2, respectively.

For zone 2 where the shear displacement of the matrix is more than d_0 and less than d_f, the traction $t_2(d)$ and the derivative of the traction matrix $t_2'(d)$ are calculated based on the following relations:

$$t_2(d) = t_m\left(1 - \frac{d - d_0}{d_f - d_0}\right) \tag{10}$$

$$t_2'(d) = \frac{-t_m}{d_f - d_0} \tag{11}$$

The energy which is the area under the CZM shape can be obtained for each zone using the following equations:

$$G_1 = \frac{t_m d_0}{2} \tag{12}$$

$$G_2 = \frac{t_m(d_f - d_0)}{2} \tag{13}$$

In order to determine d_0, the initial stiffness value (K) should be defined which is normally defined as $K = E/h_a$, where E is the Young's modulus of the adhesive and h_a is the thickness of the adhesive layer. Adding Eqs (12) and (13) gives the total area of the triangle which is considered at mode II fracture energy of the adhesive. By knowing the value of mode II fracture energy, the value of d_f can be easily obtained.

3.4. Degradation by fatigue

Fatigue failure basically takes place due to the cycle by cycle accumulation of damage. Based on the damage accumulation, the cohesive properties of the element degrade cycle

by cycle as well. Degradation of the cohesive properties of the element, changes the stress distribution and finally cause element failure. Failure of each element also changes the stress level in the remaining cohesive elements. The gradual failure of the elements causes joint failure after a specific number of fatigue cycles. Consequently, to analyze the fatigue behavior of adhesive joints, considering an appropriate degradation model is critical. The degradation models are basically semi-empirical relations which are based on the experimental results where the value of the failure parameter is a function of the number of fatigue cycles. Recently, a degradation model for mode I fatigue life estimation of adhesive material was proposed by Costa et al. [19] as follows:

$$y(N) = y_0 \left(1 - \frac{N}{N_f}\right)^k \tag{14}$$

where N and N_f are the numbers of cycles being evaluated and the cycles at failure respectively. The superscript k is the coefficient of the degradation rate which is obtained by fitting the experimental data with the numerical results. y and y_0 correspond to the property being degraded of the cohesive zone law and the initial value of that property without any degradation before the cyclic test. N_f should be already known based on the proposed method. However, by knowing the Paris law parameters, it can be obtained based on the following relation [19]:

$$N_f = \frac{\Delta a}{(da/dN)_a} \tag{15}$$

where $(da/dN)_a$ is an average value obtained from the Paris law of the adhesive, and Δa is the total length of the bonded area.

4. Data reduction method

Unlike many of classical methods, during the crack propagation the compliance based beam method (CBBM) does not require a precise crack length measurement, which is

especially useful for ENF testing, as the crack length cannot be easily monitored during the test. Because of that difficulty, error related to crack length can arise for some classical data reduction methods [20]. CBBM data reduction is based only on the specimen's compliance (C) through the test. Using beam theory, the compliance can be obtained as follows:

$$C = \frac{3a^3 + 2L^3}{8E_1Bh^3} + \frac{3L}{10G_{13}Bh} \tag{16}$$

Introducing the initial compliance C_0 and the initial crack length a_0 in the above equation, it is possible to determine the flexural modulus of the specimen.

$$E_f = \frac{3a_0^3 + 2L^3}{8Bh^3c_{0corr}} \tag{17}$$

where c_{0corr} is obtained by the following relation.

$$c_{0corr} = c_0 - \frac{3L}{10G_{13}Bh} \tag{18}$$

Unlike beam theory, in this method the different properties of the specimens are taken into account.

According to de Moura et al. [20] , a large fracture process zone is responsible for a non-negligible amount of energy dissipation. This effect can be incorporated in the CBBM approach, by applying a correction of the real crack length a_e on the compliance equation. Replacing E_f for E_1 and $a_e$for a this equation can be obtained using the following relation.

$$a_e = a + \Delta a_{FPZ} = \left[\frac{c_{corr}}{c_{corr}}a_0^2 + \frac{2}{3}\left(\frac{c_{corr}}{c_{corr}} - 1\right)L^3\right]^{1/3} \tag{19}$$

Finely, the critical fracture energy is given as

$$G_{IIc} = \frac{9P^2a_e^2}{16B^2E_fh^3} \tag{20}$$

Using this approach, the critical fracture energy, G_{IIc}, is determined from the P-δ curve and a complete R-curve can then be obtained. The only material property required is the modulus of the specimen G_{13}, which is used to determine the initial compliance.

5. Results and discussions

5.1. Experimental results

- **Static conditions**

The tests were performed at a displacement rate of 0.2 mm/min and the CBBM data reduction was used to obtain the R-curves from the load-displacement recorded during the tests.

Figure 6 shows a representative load-displacement curve obtained from an ENF test. According to Figure 6, the load initially increases with the displacement until reaching a peak, in this point the crack starts to propagate. As the tested adhesive is ductile, the decrease of the load after the peak is gradual.

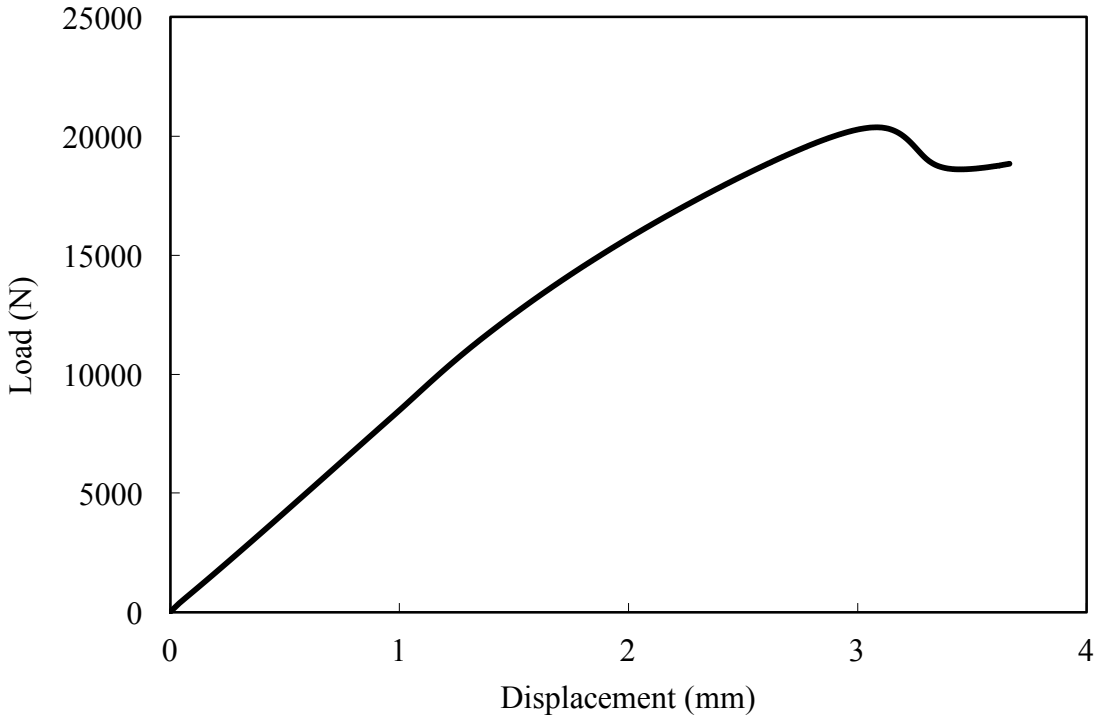

Figure 6 - Typical load-displacement curve for pure mode II

Figure 7 shows a typical resistance curve, experimentally obtained by applying CBBM. In this curve, the energy release rate value increases with the crack length. The value of the critical energy release rate was determined as the average *G* value for the slope inflexion region. This sloped region matches an equivalent crack length between 85 and 100 mm, approximately.

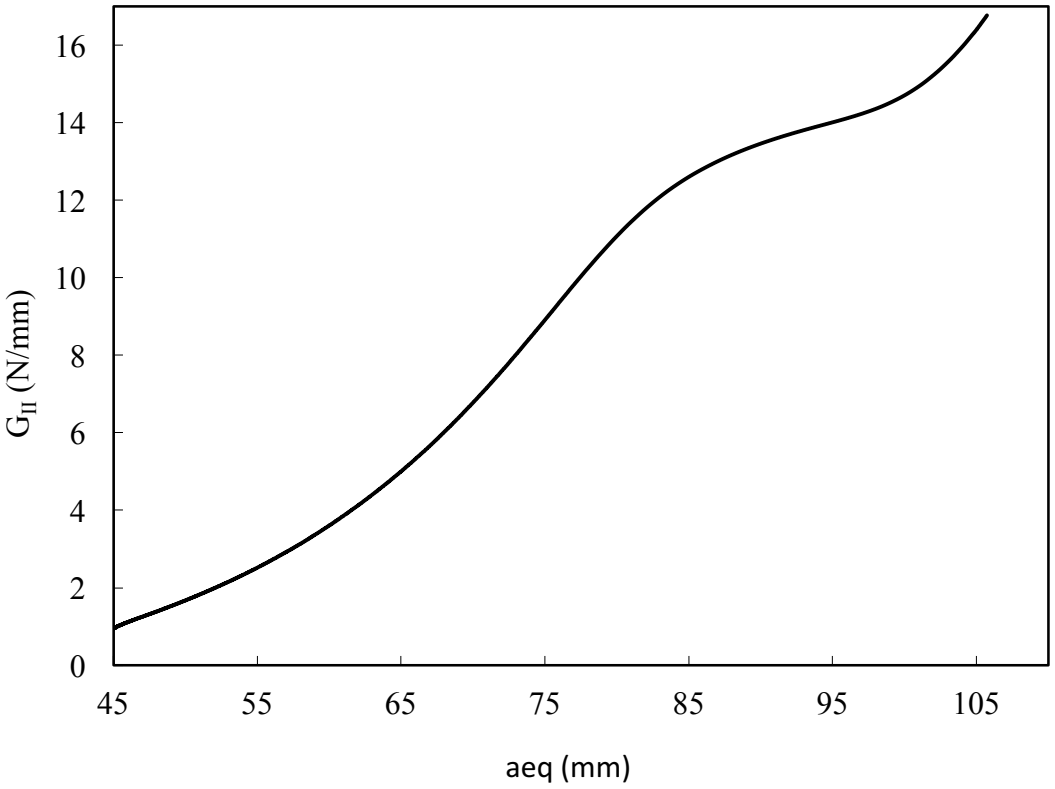

Figure 7 - Typical resistance curve for pure mode II

The failure surfaces resulting from the ENF tests were all cohesive. Figure 8 shows a representative failure surface of the specimen. The average value of G_{IIc} obtained from the experiments is 14.4 N/mm.

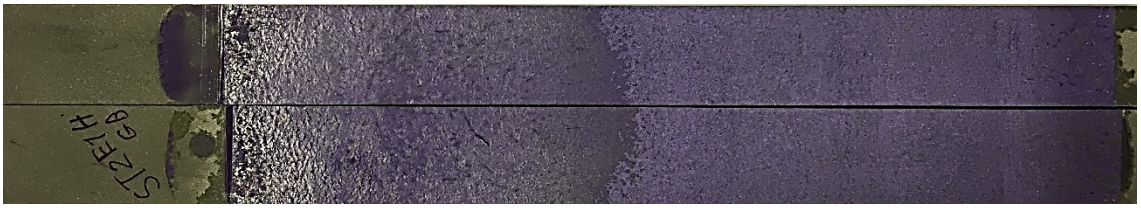

Figure 8 - Failure surface of a ENF specimen

- **Fatigue**

To determine the fatigue behavior of the adhesive in pure mode II, ENF tests were performed at 60% of maximum static strength obtained in previous section. The load ratio was set to 10%. There are different relations proposed in the literature to represent Paris law curves. Several failure parameters such as G_{max}, ΔG or normalized G_{max} (G_{max} normalized by the critical static energy release rate) are introduced with the objective of taking into account the effects of the loading conditions. Chan and Wang [21] used G_{max} normalized by the critical static energy release rate. Some authors [22, 23] have found that the use of G_{max} produces different curves for different R-ratios, while when ΔG is used, the curves collapsed into a single line regardless of R-ratio. However, the disappearance of the R-ratio effect in this case may be material dependent because others researchers have reported R-ratio effect even when ΔG was used [24, 25]. In this work, the normalized energy was considered to investigate the fatigue crack growth behavior of the adhesive. The Paris law parameters were determined by fitting a line with the experimental results. Figure 9 shows a representative curve of the load as a function of the number of cycles. Figure 10 shows how the equivalent crack evolves during the test. It is clear that the curve grows gently and gradually until a point where it begins to increase very fast until failure.

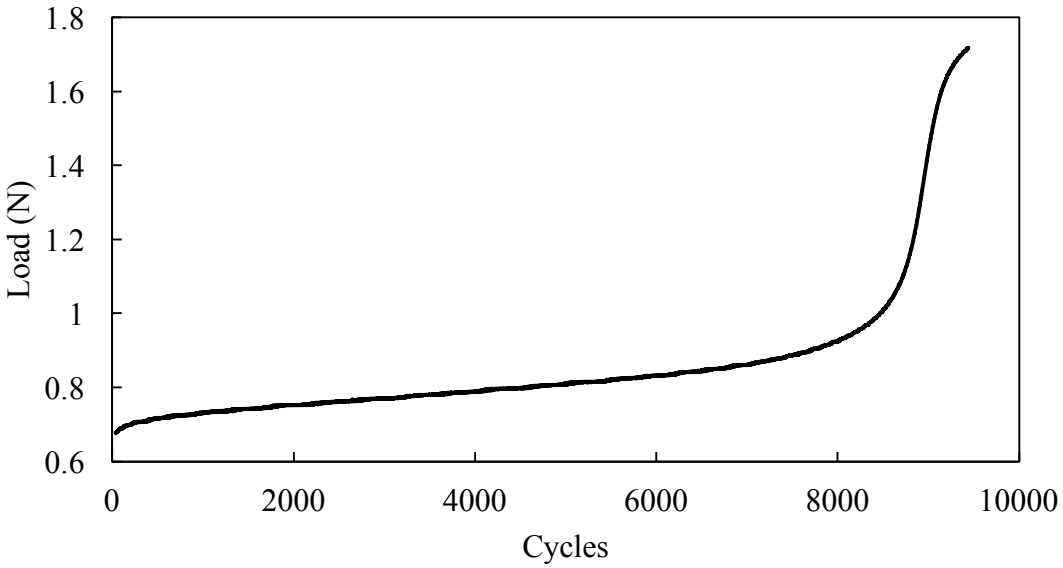

Figure 9 – Evolution of the load during the test

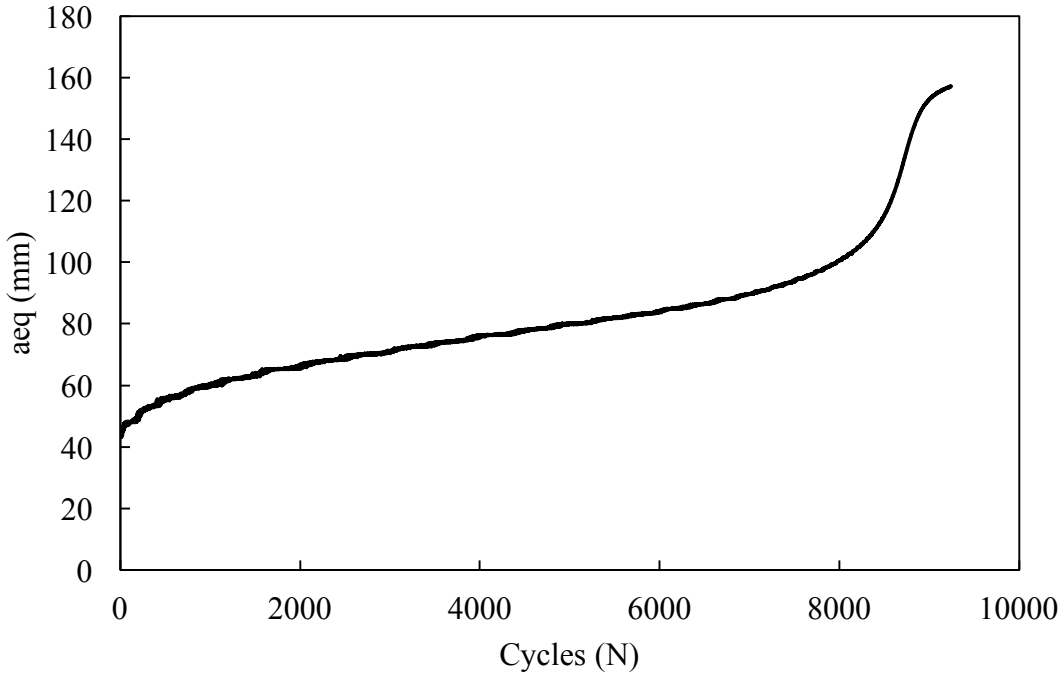

Figure 10 - Evolution of the crack equivalent during the test

Figure 11 shows the evolution of energy release rate with the equivalent crack length. As expected, the energy release rate increases until the end of the test. Because the displacement increases while the load is constant, this leads to an increase in compliance

and therefore, increases in the fracture energy values. An example of fatigue crack growth curve is shown in Figure 12, where G_{IIc} is the mode II fracture energy of the adhesive.

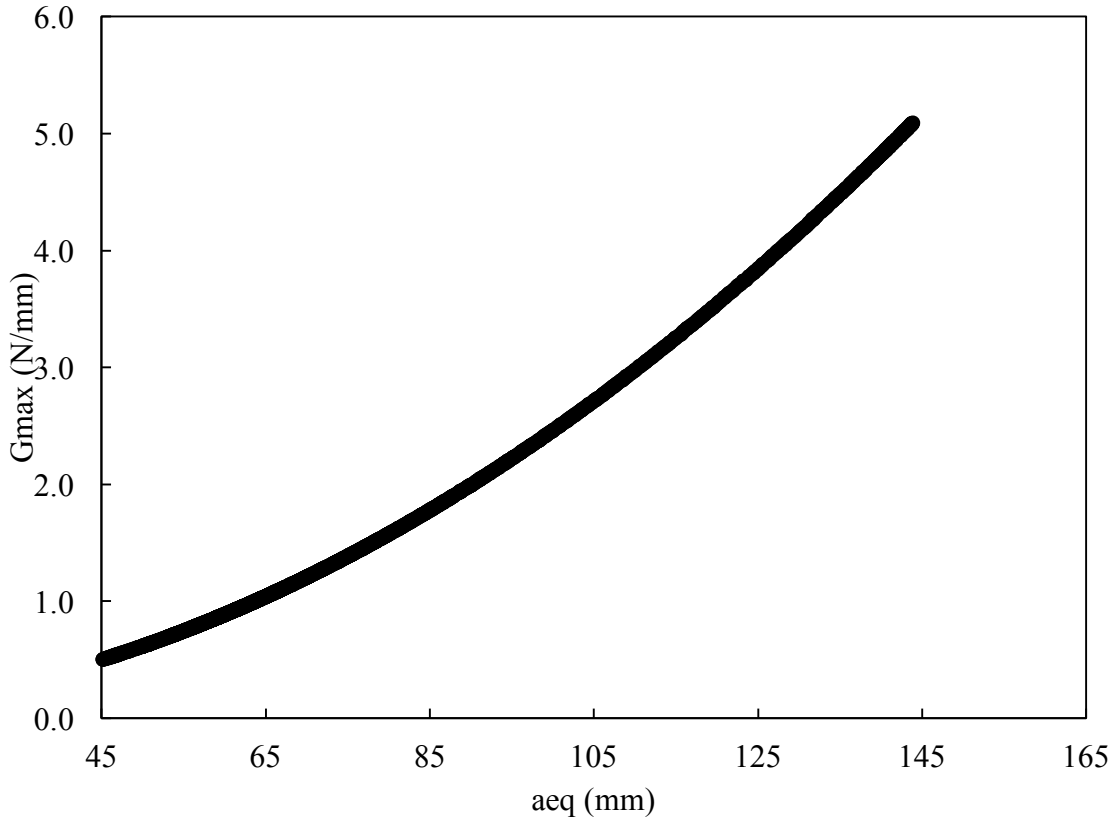

Figure 11 - Evolution of the energy release rate with the equivalent crack in an ENF specimen

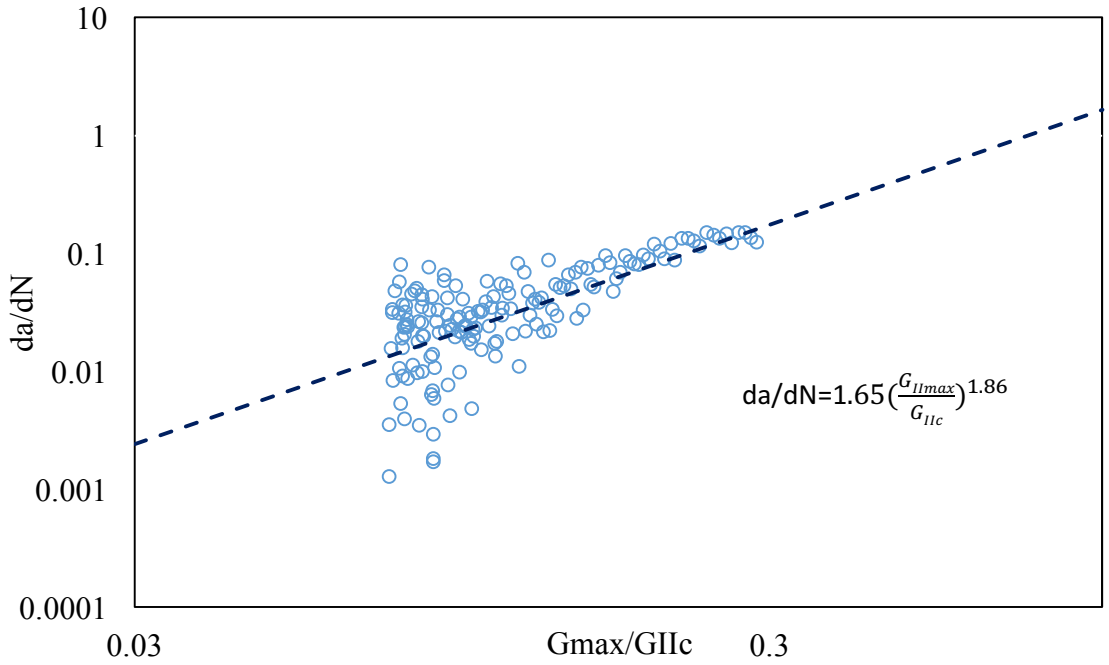

Figure 10 – A typical Paris law curve

The slope of the Paris law curve (m), which corresponds to the velocity of the crack propagation, the threshold energy (G_{th}), which indicates the energy value corresponding to the crack propagation onset and c, which is the intercept of the curve with the vertical axis are the three parameters which can be obtained by doing fatigue fracture tests. For mode II loading condition, the Paris law parameters and G_{th} were obtained for the tested adhesive (see Table 2).

Table 2 - Paris law parameters

	Nº of specimens	Intercept, c	Slope, m	Threshold	Cycles to failure
Average	5	1.59±0.11	1.91±0.17	0.10±0.02	8875±2000

- **Crack growth simulation**

The main objective of this section is to validate the already proposed mode I data degradation method for the joints which experience pure mode II loading conditions. To

achieve this, an UEL subroutine was written to degrade the traction-separation properties of cohesive elements based on the triangular CZM. In the numerical analysis, the maximum load (which in the current case is 60% of the static strength) was applied to the joint. The degradation rate was based on Eq. (14) where y_0 and y were considered as the initial traction and the value of traction for the current number of cycles, respectively. By degrading the properties of the elements, the crack propagation onsets and continues as a function of the number of cycles.

Figure 13 shows a typical Paris law curve obtained by the numerical analysis, where the crack propagation rate is shown as a function of the normalized energy. However, it should be noted that the developed method is used for total fatigue life estimation of the adhesive joint in pure mode II loading conditions and the value of *k* in Eq. 14 should be adjusted to fit the total fatigue life of the numerical with the experimental results.

The crack growth experience three different stages based on the numerical analysis like the experimental results. In the first part, the crack does not propagate until a specific number of cycles. This part corresponds to the fatigue crack initiation life of the joint. Using the current developed numerical tool, the crack initiation life can be obtained. Then the crack propagation onsets in the second stage of the numerical analysis. This section corresponds to the stable crack growth part of the Paris law. In contrast with the Paris law where the last stage of crack growth corresponds to the unstable crack propagation, the crack propagation almost stops in the last stage of fatigue life for a 3-point bending ENF test because of the presence of compressive stresses due to the applied bending load.

It should be noted that we cannot compare the crack length obtained by the numerical analysis with the experimental data where the CBMM technique is employed for measuring the crack length. As it is shown in Figure 10, using the CBBM data treatment method, the crack length increase from the beginning of the fatigue test while, in reality

for the tested joints, a major part of the fatigue life is spent for fatigue crack initiation. This difference between the CBBM results and the reality of the test is because of the concepts of the data treatment approach. CBBM as it was mentioned earlier, is based on the compliance of the joints not the measurement of the crack length during the test. Consequently, CBBM can take into account the fracture process zone for correcting the crack length which makes difference between the results obtained by experimental with the numerical. However, based on the results it was found that by choosing an appropriate value of *k* the total number of fatigue life will be fit well with the experimental data. It means that the previously proposed mode I degradation approach can be successfully applied for pure mode II loading conditions.

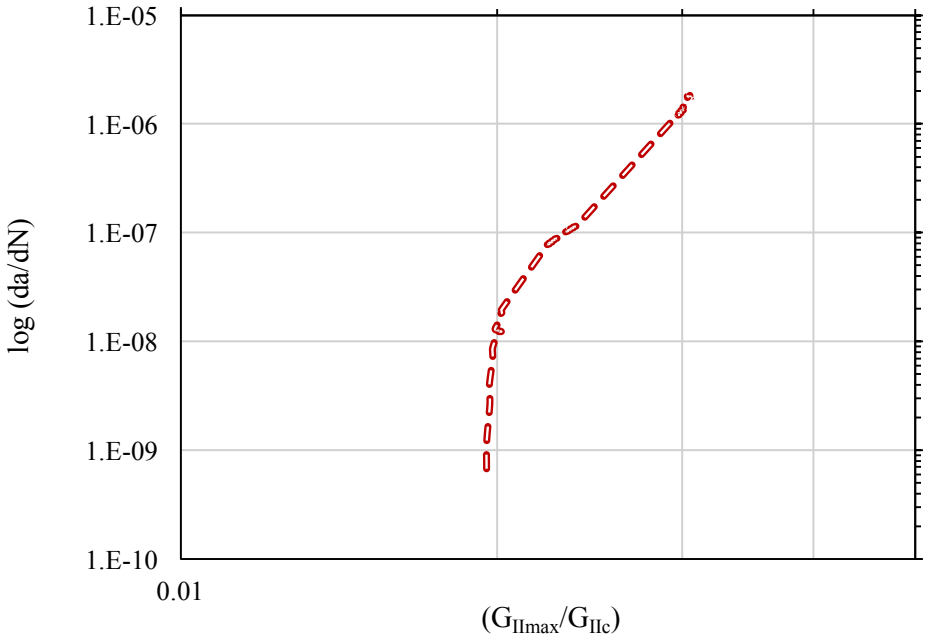

Figure 13 – A typical Paris law curve obtained by the numerical approach

Conclusions

In this study, a numerical tool was developed for fatigue life prediction of adhesive joints in pure mode II loading conditions. To achieve this, a previously published mode I data degradation approach was extended for pure mode II loading conditions. A UEL

subroutine was prepared and implemented into Abaqus to analyze the degradation of the cohesive properties of the elements based on the degradation model. The damage initiation and damage evolution were calculated based on a triangular shaped CZM.

Fatigue tests were also performed on end notched flexure (ENF) specimens to calibrate the degradation model. By adjusting the calibration parameter and fitting the experimental data with the numerical results, it was found that the degradation approach can be applied for pure mode II loading conditions as well pure mode I. As the adhesive joints are mostly designed for shear loading conditions (instead of peel stress), the introduced approach can be considered as a useful tool for fatigue life estimation of adhesive joints.

References

1. LFM. Da Silva, A. Öchsner, R.D. Adams, Handbook of adhesion technology, Springer Science & Business Media, Berlin Heidelberg, 2011.
2. D. Dugdale, Yielding of steel sheets containing slits, Journal of the Mechanics Physics of Solids, 1960, **8**(2): p. 100-104.
3. GI. Barenblatt, The mathematical theory of equilibrium cracks in brittle fracture, in Advances in applied mechanics, 1962, Elsevier. p. 55-129.
4. AD. Morais, Analysis of the fracture process zone and effective crack length in the adhesively bonded end-notched flexure specimen, The Journal of Adhesion, 2018: p. 1-26.
5. M. Gheibi, M. Shojaeefard, HS. Googarchin, Direct determination of a new mode-dependent cohesive zone model to simulate metal-to-metal adhesive joints, The Journal of Adhesion, 2018: p. 1-28.
6. G. Alfano, M. Crisfield, Finite element interface models for the delamination analysis of laminated composites: mechanical and computational issues, International Journal for Numerical Methods in Engineering, 2001, **50**(7): p. 1701-1736.
7. M. Kafkalidis, MD. Thouless, Structures, The effects of geometry and material properties on the fracture of single lap-shear joints. International Journal of Solids, 2002, **39**(17): p. 4367-4383.
8. N. Chandra, H. Li, C. Shet, H. Ghonem, Some issues in the application of cohesive zone models for metal–ceramic interfaces. International Journal of Solids, 2002, **39**(10): p. 2827-2855.
9. C. de Sousa, R. Campilho, E. Marques, M. Costa, LFM. Da Silva, Overview of different strength prediction techniques for single-lap bonded joints. Journal of Materials: Design Applications, 2017, **231**(1-2): p. 210-223.

10. K. Park, GHJE. Paulino, Computational implementation of the PPR potential-based cohesive model in ABAQUS: educational perspective, Journal Engineering Fracture Mechanics, 2012, **93**: p. 239-262.
11. H. Khoramishad, AD. Crocombe, KB. Katnam, Predicting fatigue damage in adhesively bonded joints using a cohesive zone model, International Journal of Fatigue, 2010, **32**(7): p. 1146-1158.
12. O. Nguyen, EA. Repetto, M. Ortiz, RA. Radovitzky, A cohesive model of fatigue crack growth. International Journal of Fracture, 2001, **110**(4): p. 351-369.
13. S. Maiti, P. Geubelle, A cohesive model for fatigue failure of polymers, Journal Engineering Fracture Mechanics, 2005, **72**(5): p. 691-708.
14. A. Turon, J, Costa, PP. Camanho, CG. Dávila, Simulation of delamination in composites under high-cycle fatigue, Journal Composites Part A: Applied Science, 2007, **38**(11): p. 2270-2282.
15. D. Tumino, F. Cappello, Simulation of fatigue delamination growth in composites with different mode mixtures, Journal od Compsite Materials, 2007, **41**(20): p. 2415-2441.
16. P. Robinson, U. Galvanetto, D. Tumino, G. Bellucci, D. Violeau, Numerical simulation of fatigue-driven delamination using interface elements. International Journal of Numerical Methods in Engineering, 2005, **63**(13): p. 1824-1848.
17. F. Moroni, A. Pirondi, A procedure for the simulation of fatigue crack growth in adhesively bonded joints based on a cohesive zone model and various mixed-mode propagation criteria, Journal Engineering Fracture Mechanics, 2012, **89**: p. 129-138.
18. F. Ribeiro, M. Martinez, C. Rans, Evaluation of mode II fatigue disbonding using Central Cut Plies specimen and distributed strain sensing technology, The Journal of Adhesion, 2018: p. 1-27.
19. M. Costa, G. Viana, R. Créac'hcadec, LFM. Da Silva, A cohesive zone element for mode I modelling of adhesives degraded by humidity and fatigue, International Journal of Fatigue, 2018, **112**: p. 173-182.
20. M. De Moura, RDSG. Campilho, JPM. Gon;alves, Pure mode II fracture characterization of composite bonded joints.International Journal of Solids, 2009, **46**(6): p. 1589-1595.
21. WS. Chan, AS. Wang, Free-edge delamination characteristics in S2/CE9000 glass/epoxy laminates under static and fatigue loads, in Composite Materials: Fatigue and Fracture, Second Volume, 1989, ASTM International.
22. S. Mall, G. Ramamurthy, MA. Rezaizdeh, Stress ratio effect on cyclic debonding in adhesively bonded composite joints, Journal Composite Structures, 1987, **8**(1): p. 31-45.
23. MA. Rezaizadeh, Mixed-mode cyclic debonding of adhesively bonded composite joints, 1985.
24. M. Hojo, K. Tanaka, CG. Gustafson, R. Hayashi, Effect of stress ratio on near-threshold propagation of delimination fatigue cracks in unidirectional CFRP, Journal Composites Science Techonology, 1987, **29**(4) p.273-292.
25. GL. Roderick, RA. Everett Jr, JH. Crews Jr, Cyclic Debonding of Unidirectional Composite Bonded to Aluminum Sheet for Constant-Amplitude Loading,National Aeronautics and Space Administration Hampton Va Langley Research, 1976.

Paper 2

Influence of mode mixity and loading conditions on the fatigue crack growth behavior of an epoxy adhesive

J. Monteiro[1], A. Akhavan-Safar[2], R. Carbas[2], E. Marques[2], R Goyal[3], Mohamed El-zein[4], L.F.M da Silva[1]

[1]Department of Mechanical Engineering, Faculty of Engineering of the University of Porto, Rua Dr. Roberto Frias, 4200-465 Porto, Portugal

[2]Institute of Science and Innovation in Mechanical and Industrial Engineering (INEGI), Rua Dr. Roberto Frias, 4200-465 Porto, Portugal

[3]Deere & Company, Asia Technology and Innovation Center, Pune, MH, India

[4]Deere & Company, MTIC, One John Deere Place, Moline, II. 61265, United States

Abstract

Due to their inherent advantages, the use of adhesive joints has widely increased in several industries. However, the design of these joints is not simple, as bonded connections experience mixed mode and mostly cyclic stresses conditions during their service life. The aim of the current research is to investigate the fatigue and fracture behavior of a structural epoxy adhesive. Double cantilever beam (DCB) and end-notched flexure (ENF) tests were carried out to determine mode I and mode II fatigue and fracture behavior of an epoxy-based adhesive. For the mixed mode condition, an apparatus was used to obtain the mixed mode results. The energy release rate was calculated considering an equivalent crack length approach, called compliance based beam method (CBBM). The effects of load level and load ratio on the mode I fatigue crack growth (FCG) behavior and Paris law parameters were also investigated. Result showed that the effect of load level on fatigue crack propagation is more pronounced for lower *R*-ratios. According to the experimental data, when the crack faces are closer during the unloading process, the difference between the R^2 and G_{min}/G_{max} is higher. Some reasons for this behavior are

the crack closure phenomenon, difficulty in measuring the G_{min} and also the employed data reduction approach.

Keywords: Adhesive joint, Fatigue loading, Paris law, R ratio, Mixed mode.

1. Introduction

During the past decades, the use of adhesives as a structural bonding component has significantly increased in a wide range of industries such as the automotive, aerospace, and aeronautical [1]. The use of adhesive as a structural bonding component offers a more uniform stress distribution over the bonded area, avoids stress concentrations, reduces the weight, allows to bond dissimilar materials and confers some flexibility to the joint, making it able to withstand stronger dynamic loads [1]. Within this context, it is crucial to study the behavior of adhesive joints when subjected to fatigue loading conditions. However, the exact prediction of the fatigue life is quite difficult due to the complex behavior that polymeric materials, such as adhesives, exhibit under loading and unloading cycles.

Usually, fatigue lifetime can be divided into two main phases, known as crack initiation and crack propagation. The fatigue crack propagation relates the fracture parameter (such as maximum strain energy release rate G_{max}) with the crack growth rate (*da/dN*). Some authors [2, 3] studied the effect of the load ratio on the fatigue behavior of adhesively bonded joints using experimental and numerical approaches. They observed that increasing the load ratio for a constant maximum fatigue load increases the fatigue life. Some studies dealt with the effect of the load ratio. Kawashita et al. [4] concluded that the crack growth rate decreases with increasing load ratio, however, Hoja et al. [5] observed that increasing the load ratio increases the crack growth rate. Rans et al. [6], based on results already published in [4, 7, 8] observed that there are large differences in

the load ratio effect on the fatigue crack growth (FCG) for different loading modes. Some studies have been dedicated to the effect of mode mixity [9]. Azari et al. [10] studied the FCG behavior of adhesive joints under mode I and mixed mode loadings. In order to predict fatigue failure of adhesive joints, Pirondi et al. [11] applied a fracture mechanics-based model. Effects of the environmental, mean stress, surface treatment and also the surface profile on fatigue behavior of adhesive joints have been addressed in some studies [12-15].

These results indicate that the fatigue behavior of bonded joints is mostly a function of the adhesive type and loading conditions, although other parameters, such as the method of data treatment, may affect the experimental data. The aim of this study is to investigate the fatigue fracture behavior of an epoxy adhesive using the Paris law and by employing the CBBM approach. By measuring the minimum fracture energy for each loading cycle, the effects of loading conditions on the ratio of G_{min}/G_{max} were also studied.

2. Experimental details

In the experimental procedure of this work, specimens with the same geometry were manufactured and tested according to DCB, ENF and mixed mode loadings. The tests were performed both in static and fatigue conditions. The main objective of these tests was to obtain the fracture energy, the fracture envelope and the FCG behavior of the adhesive as a function of mode mixity.

2.1. Materials

A high performance one-component structural epoxy based paste was considered as adhesive to bond steel substrates. The main application of the adhesive is for metal bonding where higher impact resistance, durability and stiffness is required.

Tensile bulk and thick adherend shear test (TAST) tests were used to determine the tensile and shear properties of the adhesive (see Table 1). Figure 1 shows a typical tensile stress-strain curve of the adhesive. High strength steel was used as substrates. The mechanical properties of the substrates are given in Table 1.

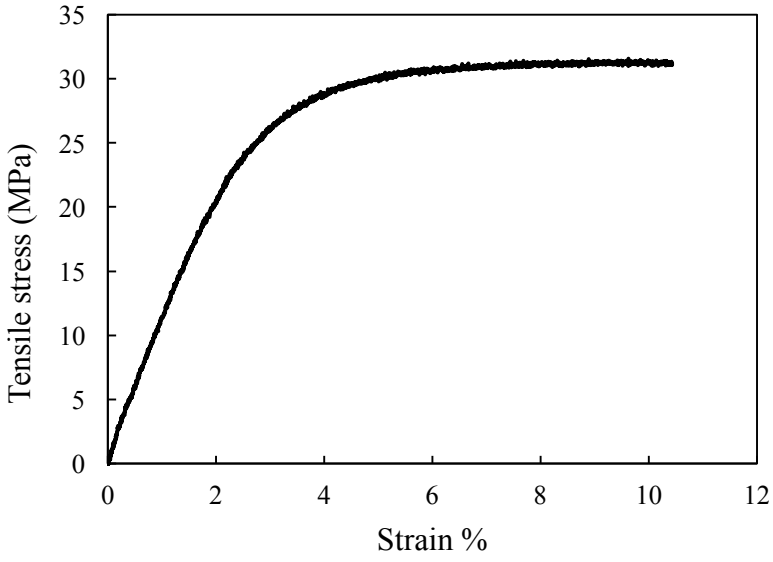

Figure 1 - Typical tensile stress-strain curve

Table 1 - Mechanical properties of the adhesive and the substrate

Properties	Substrate	Adhesive
Tensile strength (MPa)	-	31.3±0.6
Tensile strain to failure (%)	-	10.4±0.5
Shear strength (MPa)	-	23.1±0.5
Shear strain to failure (%)	-	43.3±0.9
Young's modulus (MPa)	210000	1159±29.3
Shear modulus (MPa)	-	440±8.7
Poisson's ratio (ν)	0.3	

2.2. Joint geometry and preparation

As the DCB, ENF and mixed mode tests use a DCB type specimen, the same specimen geometry was used for all the loading conditions, simplifying the manufacturing process. Figure 2 shows a schematic of the tested joints. In order to ensure a bondline thickness of 0.3 mm, calibrated metal spacers were positioned at both ends of the joint. To guarantee

a consistent pre-crack size (45 mm) of the specimens, a thin blade was used. A hot-plate press was used to control both the temperature and pressure of the curing process. Following the manufacturers datasheet, the cure time and the temperature were set to 20 min and 177ºC respectively. The pressure was equal to 25 bar during the curing process. To avoid the influence of the excess of adhesive on the results, after curing, the lateral surfaces of the specimens were cleaned with sandpaper. Before testing was carried out, all specimens were kept at room conditions for 72 h. To promote stable crack propagation during the actual test, the specimens were submitted to a pre-cracking process (slowly loaded until crack initiation occurs) and the blades were removed before the test.

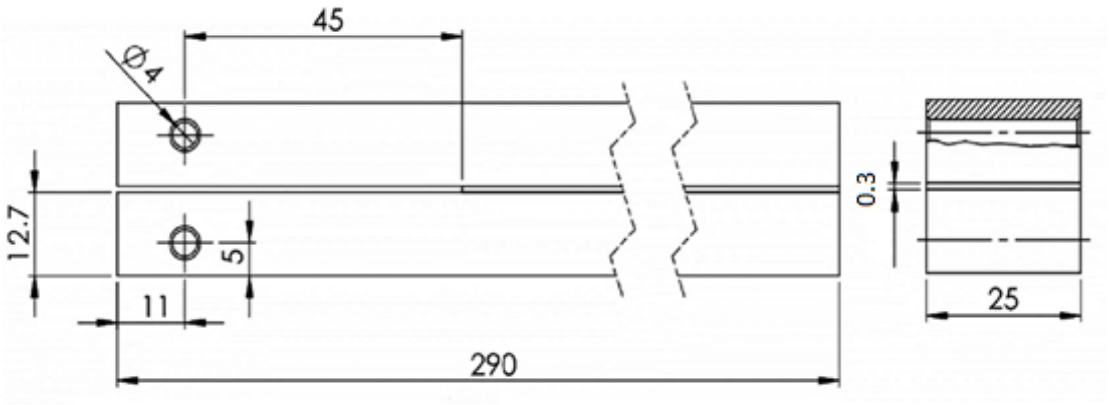

Figure 2 - Specimens geometry according to ASTM D-3433-99 (dimensions in millimeters) adapted from [16]

2.3. Testing conditions

DCB, ENF and mixed mode (45^{o}) tests were performed under quasi static condition at room temperature with a displacement rate of 0.2 mm/min. Table 2 displays the different conditions used for the fatigue tests for mode I, mode II and mixed mode.

To overcome the existing difficulties of measuring mixed mode fracture toughness, an apparatus was developed by the *ADFeup* group [17]. This apparatus does not need crack length measurements, instead, two linear variable differential transformer (LVDT) are used to measure displacement. The apparatus is presented in Figure 3

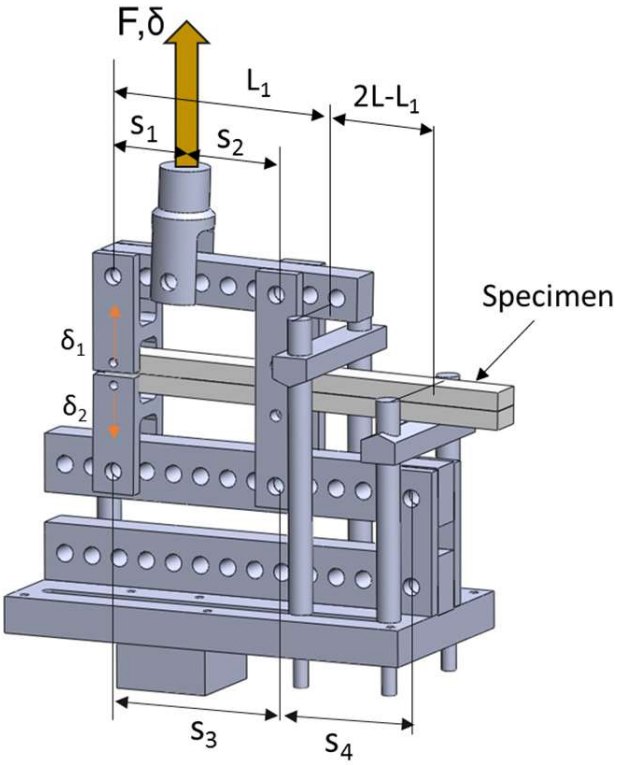

Figure 3 - scheme of the mixed mode apparatus used

Changing the beam lengths (s_1, s_2, s_3 and s_4) the apparatus can be configured for multiple phase angles between pure mode I and II. This phase angle and the forces applied to the top and bottom arms of the specimens change according to the beam lengths, the angle is given by:

$$\varphi_{apparatus} = \tan^{-1} \frac{\sqrt{3}\left(\frac{F_1}{F_2} + 1\right)}{2\left(\frac{F_1}{F_2} - 1\right)} \quad (1)$$

The load applied through the apparatus is a combination of mode I and mode II. Figure 4 shows how the apparatus setup can be decomposed in mode I component (DCB) and mode II (ENF).

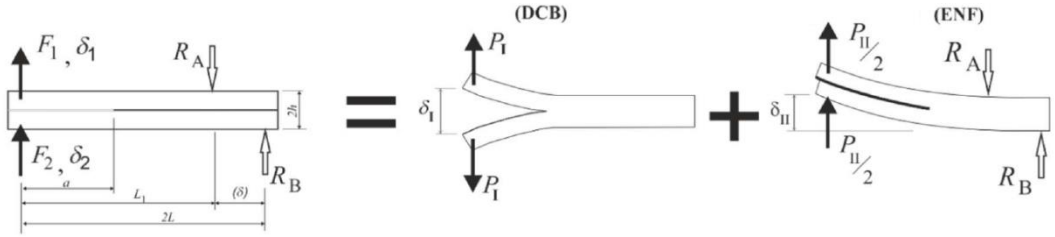

Figure 4 - Schematic representation of the specimen loading with mode I and mode II partition [18]

The load applied by the machine is decomposed in two, corresponding to the top and bottom loads, F_1 and F_2 respectively (see Figure10). The relation is given by:

$$F_1 = F\frac{s_1}{s_3};\ F_2 = F\frac{s_1 s_4}{s_3(s_3+s_4)} \tag{2}$$

Mode I and mode II load components, P_I and P_{II} are determined by:

$$P_I = \frac{F_1 - F_2}{2};\ P_{II} = F_1 + F_2 \tag{3}$$

Table 2 - load conditions used in fatigue tests

	nber of specimens	d level of quasi-static load	Load ratio
Mode I	5	60%	10% and 30%
	2	40%	10% and 30%
	1	35%	30%
		30%	
Mode II	5	60%	10%
lixed mode	5		

As a part of the experimental program, the effect of load level and R ratio on fatigue crack propagation behavior of the adhesive were studied for mode I loading condition (see Table 2).

3. Data reduction method

Unlike many of the classic methods, CBBM does not require crack length measurement during the test, which is an advantage of CBBM since these measurements are not easy to register in practice [19]. CBBM data reduction is based only on the specimen's compliance. According to [19], a large fracture process zone is responsible for a non-negligible amount of energy dissipation. This effect is incorporated in the CBBM formulation. Using CBBM, the critical fracture energy for pure mode I is given as follows:

$$G_{Ic} = \frac{6P^2}{B^2h^3}\left(\frac{2a_{eq}^2}{E_f} + \frac{h^2}{5G_{13}}\right) \quad (1)$$

where G_{13} is the modulus of the specimen, which is a function of the of the initial compliance and is the only material property required. E_f is the flexural modulus of the specimen and a_{eq} is the equivalent crack length. The relation for mode II is as follows:

$$G_{IIc} = \frac{9P^2a_{eq}^2}{16B^2E_fh^3} \quad (2)$$

For mixed mode tests, the fracture energy is partitioned into mode I and mode II components.

Mode I given as follows:

$$G_I = \frac{6P_I^2}{B^2h^3}\left(\frac{a_{eqI}^2}{E_f} + \frac{h^2}{5G_{13}}\right) \quad (3)$$

and mode II is as follows:

$$G_{II} = \frac{9P_{II}^2 a_{eqII}^2}{16B^2E_f h^3} \quad (4)$$

4. Results

4.1. Static test results

Figures 5 and 6 show a typical load-displacement (P-δ) curve and a typical R-curve for mode I.

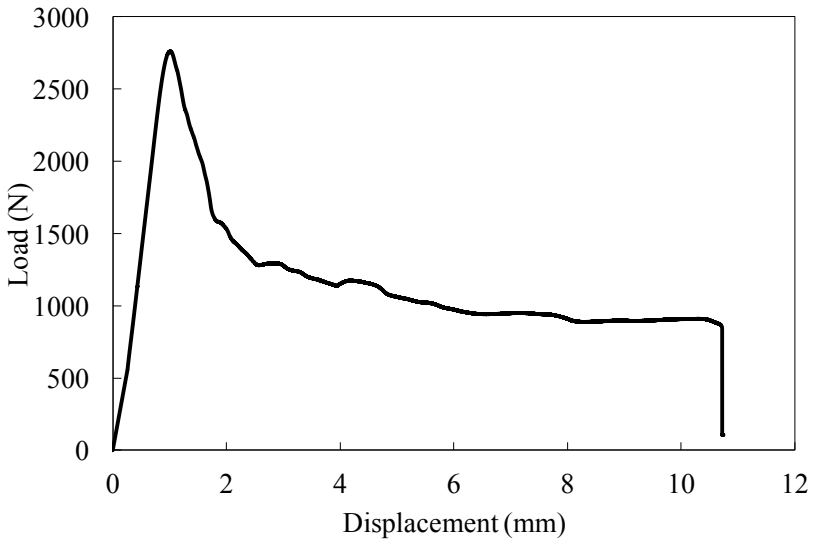

Figure 5 - Representative load-displacement curve for a DCB test

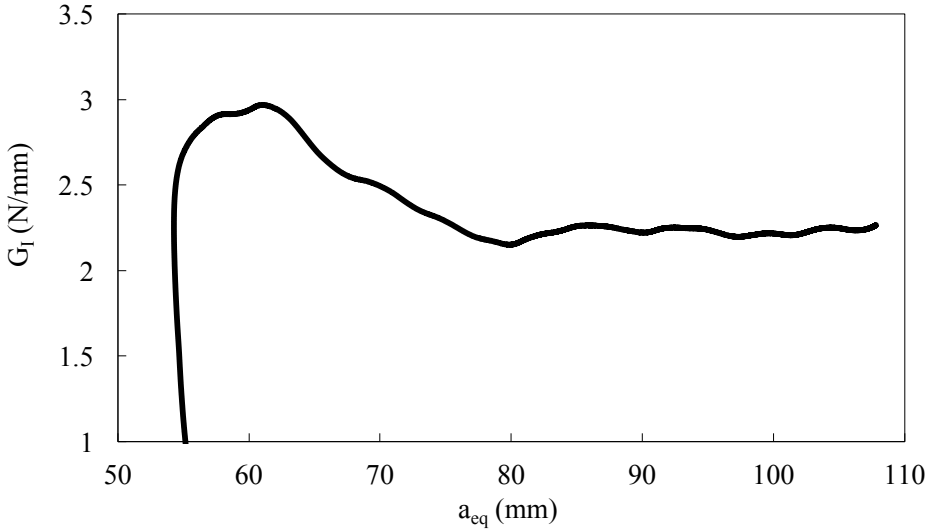

Figure 6 - Representative R-curve for a DCB test

Based on Figure 6, the energy release rate increases with the equivalent crack length, until it reaches a plateau. The value of G_{Ic} corresponds to the plateau value and is given in Table 3. Figure 7 shows a representative *P-δ* curve for a mode II loading condition. Because of the ductility of the tested adhesive, the decrease of the load after the peak is smooth.

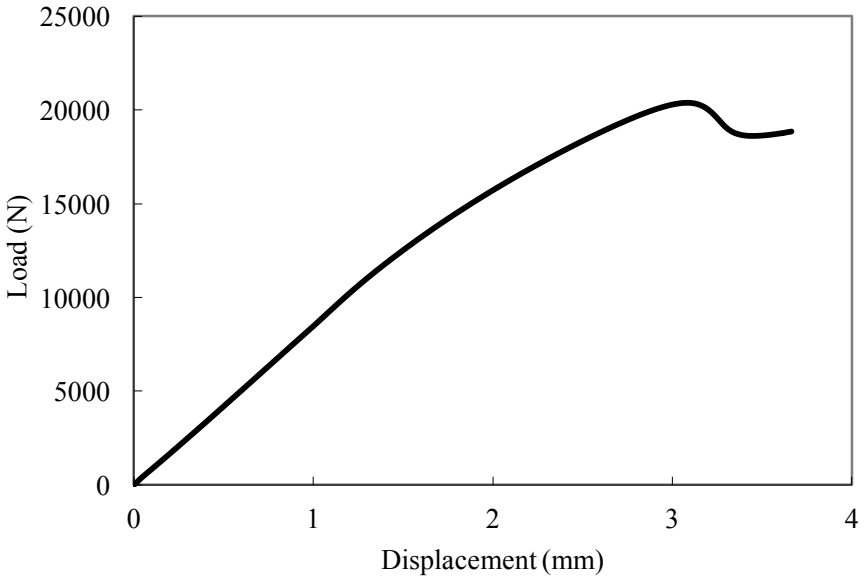

Figure 7 - Representative load-displacement curve for a ENF test

As shown in Figure 8, the energy release rate value increases with the crack length for mode II conditions. The average *G* value for the slope inflexion region corresponds to the critical energy release rate (G_{IIc}) and is represented in Table 3. This region corresponds to an equivalent crack length between 85 and 100 mm, approximately.

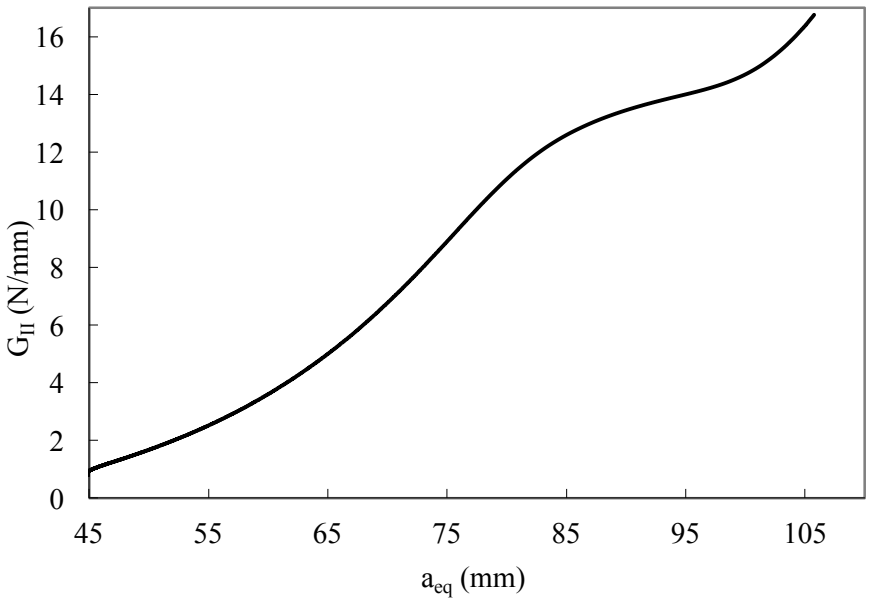

Figure 8 - Representative R-curve for an ENF test

For mixed mode tests, the fracture energy was obtained using the mixed mode testing apparatus [17, 20] where the applied load was decomposed in mode I and II components. The displacement of each beam of the specimen was recorded using two LVDTs. Figure 9 shows the *P-δ* curve for mode I and mode II components of mixed mode condition.

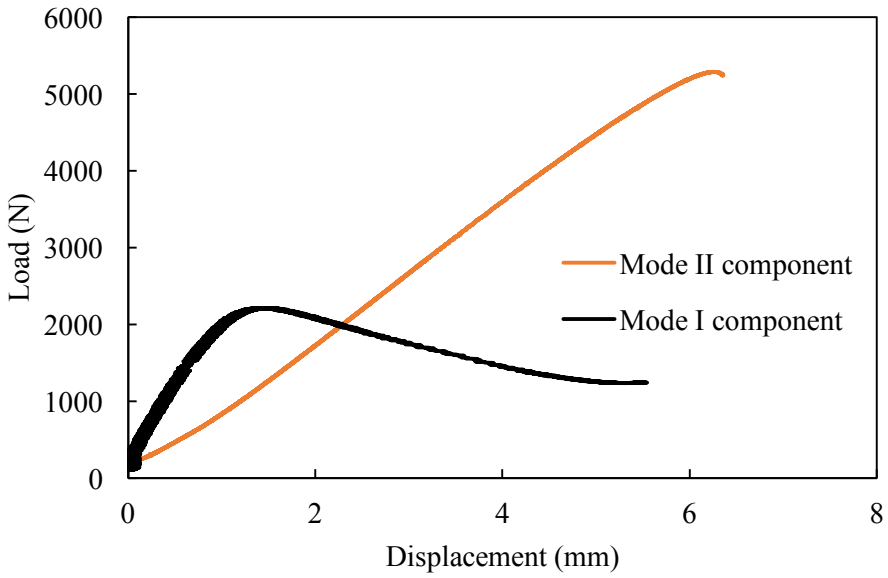

Figure 9 - Representative load-displacement curve for mode I and mode II components of mixed mode test

In Figure 10, the resulting *R*-curves for the mixed mode ratio of 45° are shown. The energy release rate value corresponds to the average values of the more stable region of the curves.

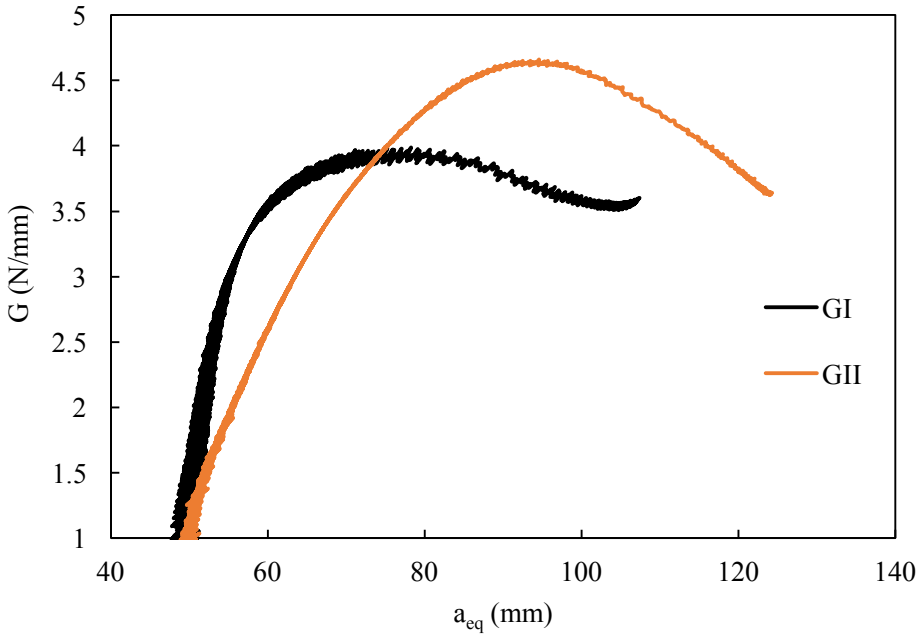

Figure 10 - Representative R-curve for a mixed mode test

For the tested phase angle (φ=45°) a similar value of the critical energy release rate for both modes was expected. The effective mixed mode angle was evaluated using G_I and G_{II}. The experimental angle calculated using G_I and G_{II} was 47.7°, which is very close to the angle defined. Table 3 displays the resulting energy release rates for pure mode I, pure mode II and the mixed mode components (mode I and mode II). For all the tested conditions, the failure type was cohesive.

Table 3 - Fracture energies of mode I, mode II and mixed mode

DCB	ENF	Mixed mode (φ=45°)	
G_{Ic}(N/mm)	G_{IIc}(N/mm)	G_I(N/mm)	G_{II}(N/mm)
2.2 ± 0.02	14.4 ± 0.8	3.9 ± 0.3	4.6 ± 0.1

Using the fracture energies presented in Table 3 fracture envelope of the tested adhesive was produced (see Figure 11).

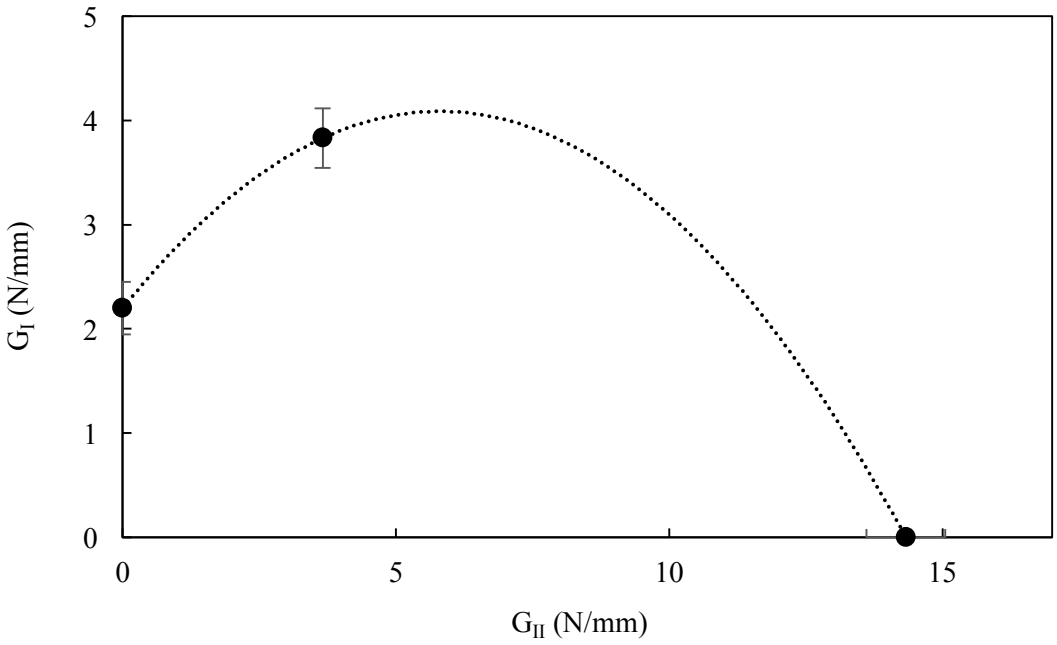

Figure 11 - Fracture envelope

4.2. Fatigue

The FCG curves were obtained using a CBBM data reduction approach to calculate the energy release rate and the equivalent crack length. Figure 12 shows a typical maximum fracture energy as a function of the corresponding crack length. According to Figure 12, the energy release rate increases until the end of the test, because the load is constant while the displacement increases, leading to an increase of the compliance and consequently, an increase in fracture energy values.

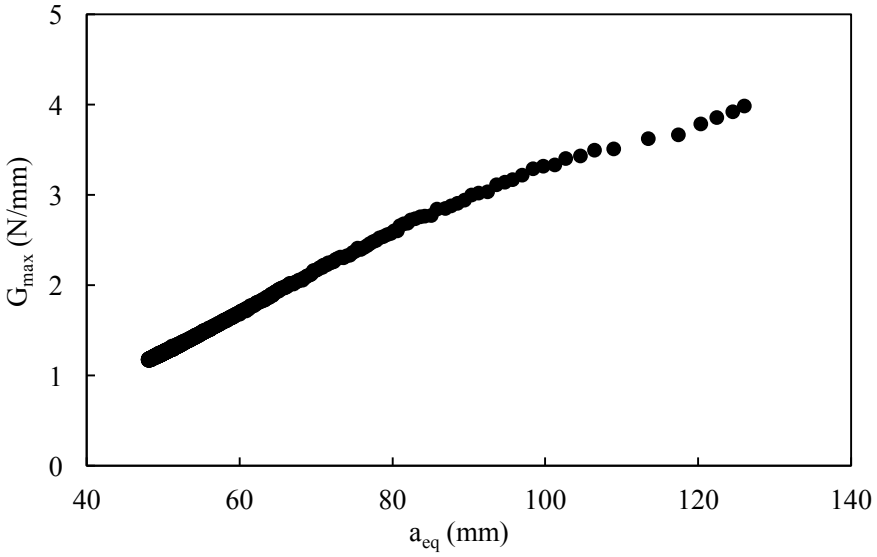

Figure 12 - Evolution of the energy release rate with the equivalent crack length for 60% of the load R-ratio 0.1

-Mode I fatigue results

Figure 14 shows two typical FCG curves for pure mode I with different load levels where the *R*-ratio was set to 0.1. As expected, higher load level and amplitude lead to a faster crack propagation and a shorter life. Similar results were obtained for joints tested with an *R*-ratio of 0.3. However, based on the experimental data it was observed that the effect of load level on fatigue crack propagation is more pronounced when the *R*-ratio is lower. Based on the experimental results it is concluded that the fatigue crack propagation life increases by decreasing the load level and increasing the load ratio. Similar results were already obtained by some other authors [3].

For the fatigue tests carried out at load levels of 30% and 35% of the maximum static strength, the crack did not propagate after more than 2.6 million cycles. However, to measure the effect of fatigue loading on the static residual fracture energy of the joints, the fatigue tests were stopped and a mode I static fracture test was performed on the

mentioned DCBs. Figure 13 shows the critical energy release rate determined on the static part and the same energy for the specimens tested after being submitted to fatigue tests.

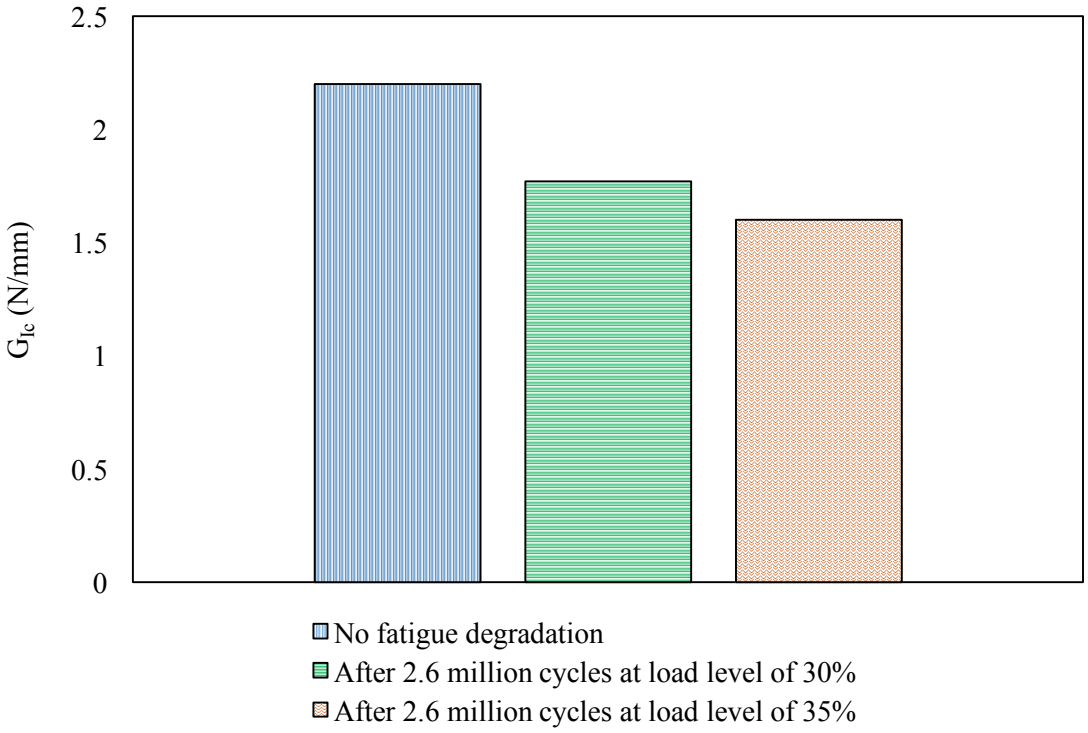

Figure 13 - Residual energy of the specimens after fatigue degradation

Although the life was considered infinite for the fatigue tests with 30% and 35% of the failure load, a small degradation of the critical energy release rate is observed after 2.6 million cycles. The degradation is higher for the specimens tested in fatigue with higher load percentage.

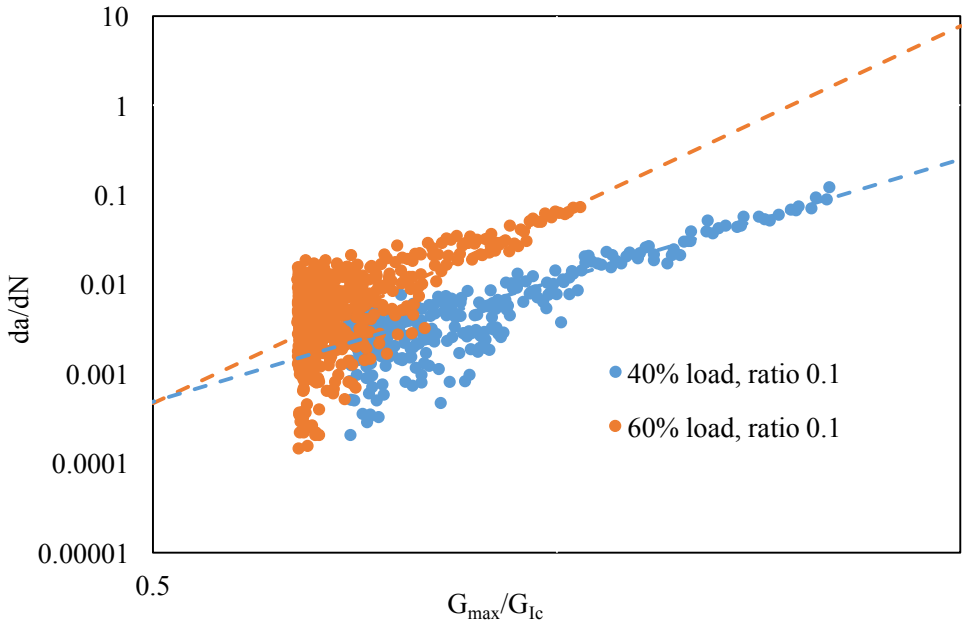

Figure 14 - Mode I Paris law for different load levels with load ratio of 0.1

The average values of the Paris law parameters obtained from the DCB tests are presented in Table 4. Figure 17 shows typical Paris law curves for pure mode I where the load level is similar but the R-ratio is different. Higher R-ratio for the same load level corresponds to a higher average load, however, the results show that, for higher R-ratio, the slope of the curve is lower and consequently the rate of FCG is lower as well. The effect of R-ratio on FCG has been described in several research works. In some studies, it was reported that higher R-ratio leads to a higher crack propagation rate [5], while in other researches, lower crack evolution has been observed by increasing the value of R-ratio [4]. However, the Paris law constants are a function of the considered failure parameters. In the current work, the normalized energy (maximum energy per cycle normalized by the static fracture toughness) is considered for obtaining the Paris law parameters. Similar relations were also employed by [21-23]. However, to take into account the effects of R ratio, some relations based on R were proposed in literature [22]. However, as the reality

of FCG is not fully known the proposed relations are mainly functions of loading conditions or material properties.

Several corrections have been applied on the primary version of the Paris law to take into account the effects of different loading conditions on fatigue crack growth behavior of materials. One of the critical factor which affect the fatigue fracture of the materials is the R ratio. Based on some literature, the effect of R ration can be taken into account by adding both G_{min} (minimum fracture energy per cycle) and G_{max} (maximum fracture energy per cycle) to the Paris law relation. They believe that the ratio of G_{min}/G_{max} is equal to R^2 [24]. The mentioned relation was investigated for the tested material. In the present study, and as it is shown in Figures 15 and 16 that the obtained values of G_{min}/G_{max} are different from R^2. A possible reason for the difference between G_{min}/G_{max} and R^2 is the crack closure phenomenon. Based on Figures 15 and 16, it was found that by increasing the load level at similar R ratio, the difference between G_{min}/G_{max} and R^2 increases. On the other hand, by keeping the load level constant and increasing the R ratio it was observed that the difference between G_{min}/G_{max} and R^2 decreases. Based on the observations, when the crack faces are closer during the unloading cycles, the difference is higher. It should be noted that crack closure phenomenon is observed in fatigue loading even when the loading condition is tension-tension. In some previously published work, such as [25], the effect of crack closure is taken into account by considering the crack closure fracture energy. However, calculation of the crack closure phenomenon is quite difficult and requires assessment by experimental methods. Another possible reason for the difference between R^2 and G_{min}/G_{max} is the difficulty in measuring G_{min} during the unloading cycles. The data reduction approach considered in the present study is also another possible reason for the difference between the G_{min}/G_{max} and R^2. CBBM considers the effects of fracture

process zone by using an equivalent crack length. However, using different data treatment methods will yield different values for the fracture energy.

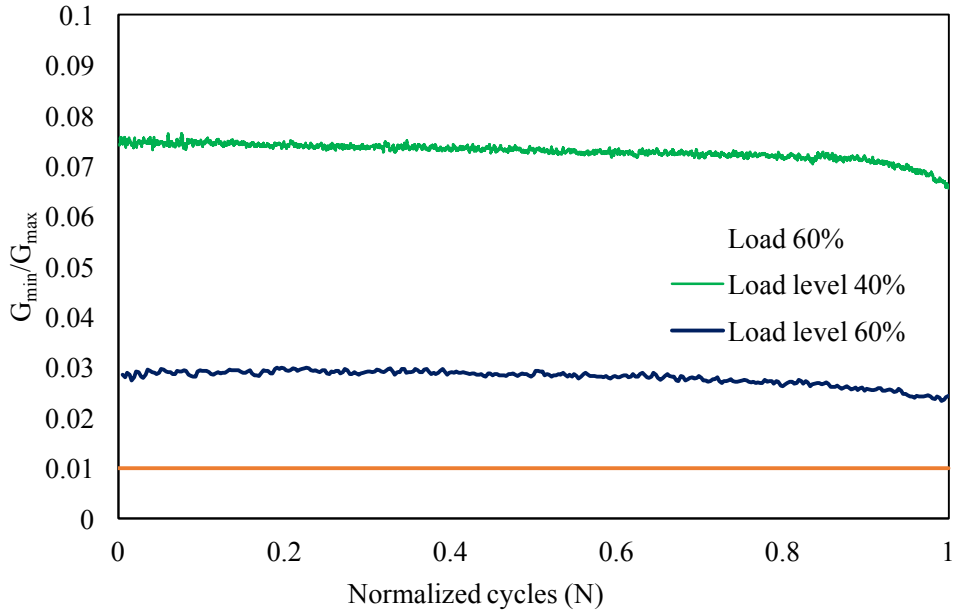

Figure 11 – R^2 vs G_{min}/G_{max} at R=0.1

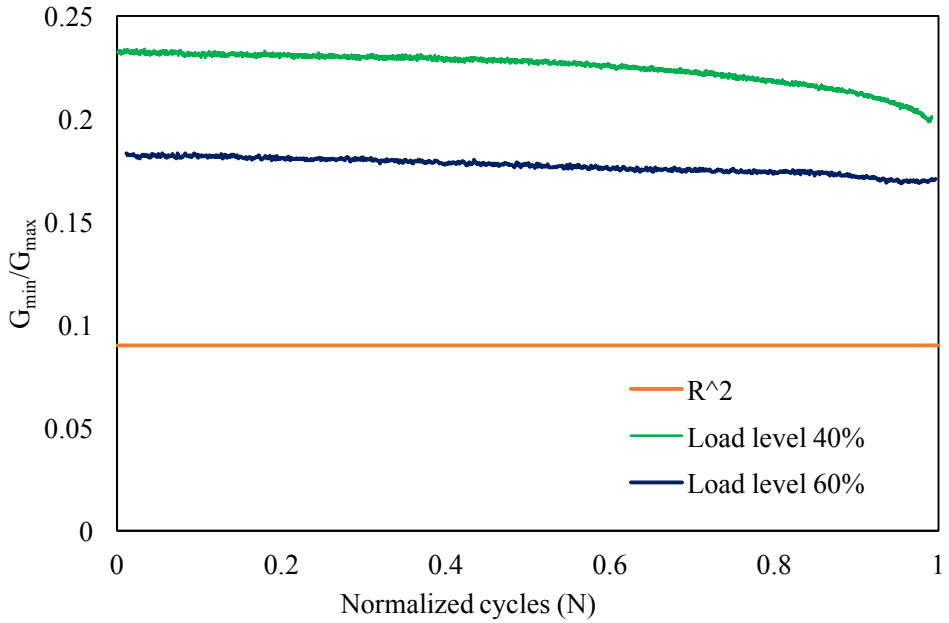

Figure 16 – R^2 vs G_{min}/G_{max} at R=0.3

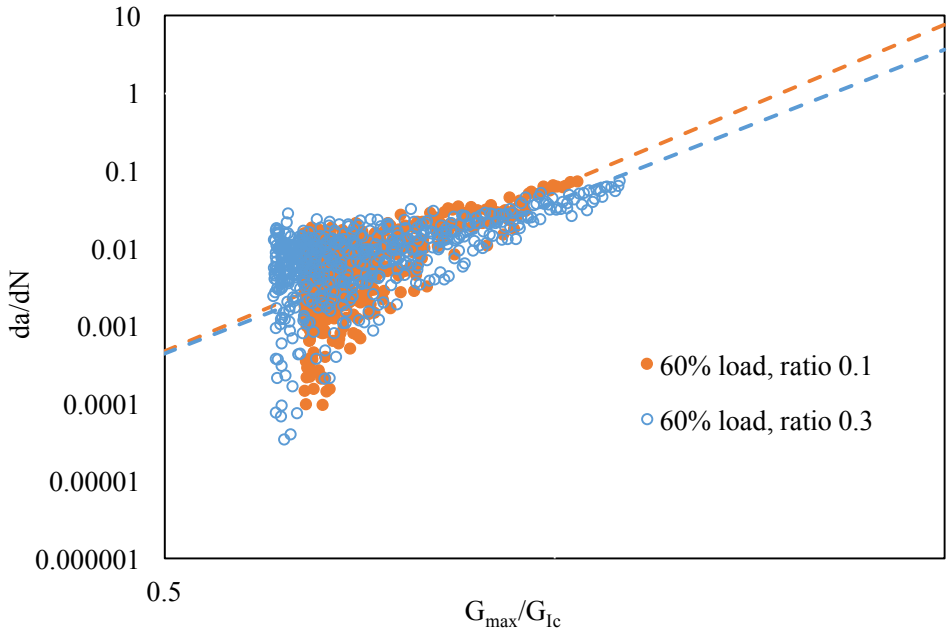

Figure 17 - Mode I Paris law curves for the same load level with different load ratios

The threshold fracture energy (G_{th}), as a critical parameter in fatigue analysis was also obtained for different loading conditions. Based on the obtained experimental data for mode I, it was found that, despite the Paris law parameters, the threshold fracture energy (G_{th}) can be considered as constant for different mode I loading conditions (see Table 4). However, by changing the mode mixity, it was observed that G_{th} is in fact a function of the mixed mode condition.

Table 4 - Paris law parameters for pure mode I

Load level of quasi-static (%)	Load ratio (%)	Intercept, c	Slope, m	G_{th}
60	10	0.057 ± 0.01	7.82 ± 0.39	0.69 ± 0.11
	30	0.055 ± 0.01	6.75 ± 0.56	0.71 ± 0.06
40	10	0.011 ± 0.001	4.55 ± 0.05	0.72 ± 0.02
	30	0.001	4.50	0.72

4.2.1. Mode II

The relation between the G_{max} and the equivalent crack length for a typical ENF fatigue test is shown in Figure 18, where it is clear that, by increasing the equivalent crack length, the energy release rate increases until the end of the test. This increase in fracture energy is due to the increasingly higher displacements that occur as the test progresses. This leads to an increase of the compliance and therefore, an increase in fracture energy.

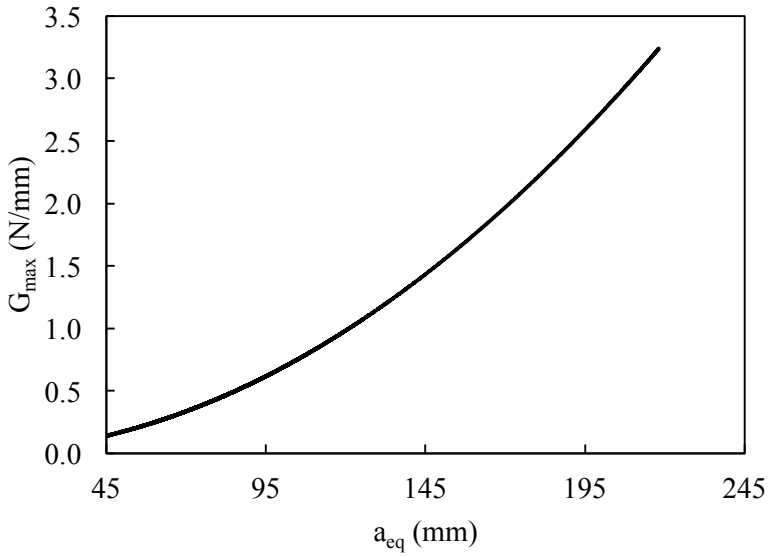

Figure 18 - Evolution of the energy release rate with the equivalent crack for an ENF test

Figure 19 depicts an example of FCG curve for pure mode II.

Figure 19 - Paris law curve for pure mode II

The Paris law parameters and G_{th} for mode II condition are given in Table 5.

The slope value for pure mode II is significantly lower than mode I, which means that the crack propagation rate in mode II is much lower than mode I.

Table 5 - Paris law parameters for pure mode II

Load level of quasi-static strength	Load ratio (%)	Intercept, c	Slope, m	G_{th}
60 %	10	1.59±0.11	1.91±0.17	0.10±0.02

4.2.2. Mixed mode

Using the data provided by the mixed-mode testing apparatus and using the CBBM, the load and displacement curves were separated to obtain mode I and mode II components of the mixed mode tests. By having the two components calculated independently, it becomes possible to determine the Paris law curves, using the same procedure as employed for the pure modes.

The FCG determined in this case showed well-defined curves for the mode I and mode II components due to the fact that the phase angle is located well in the middle of the two pure modes.

Representative curves obtained for mode I and mode II components of the mixed mode tests are presented in Figures 20 and 21, respectively.

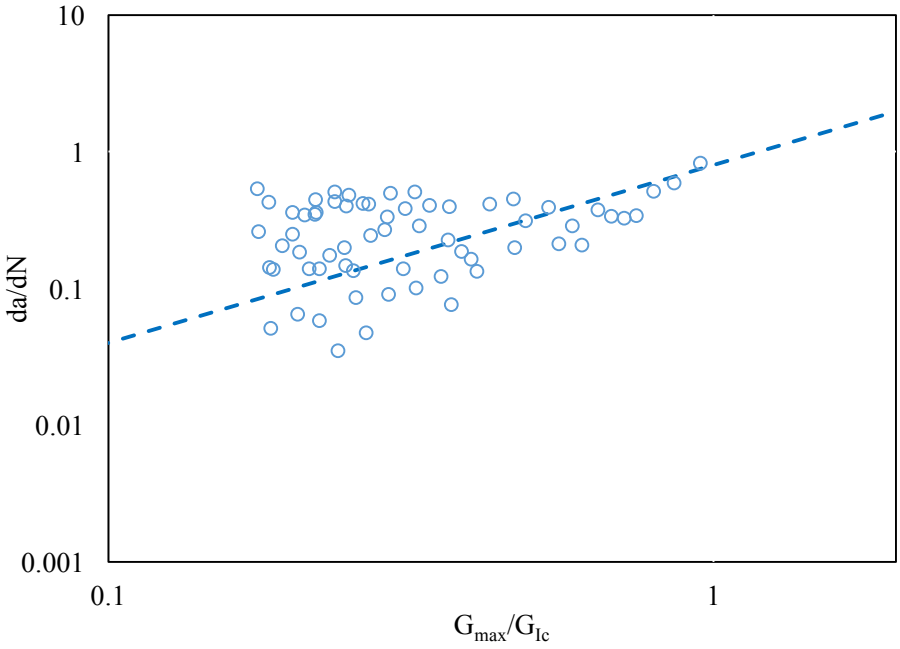

Figure 20 - Mode I component for mixed mode test (φ=45°)

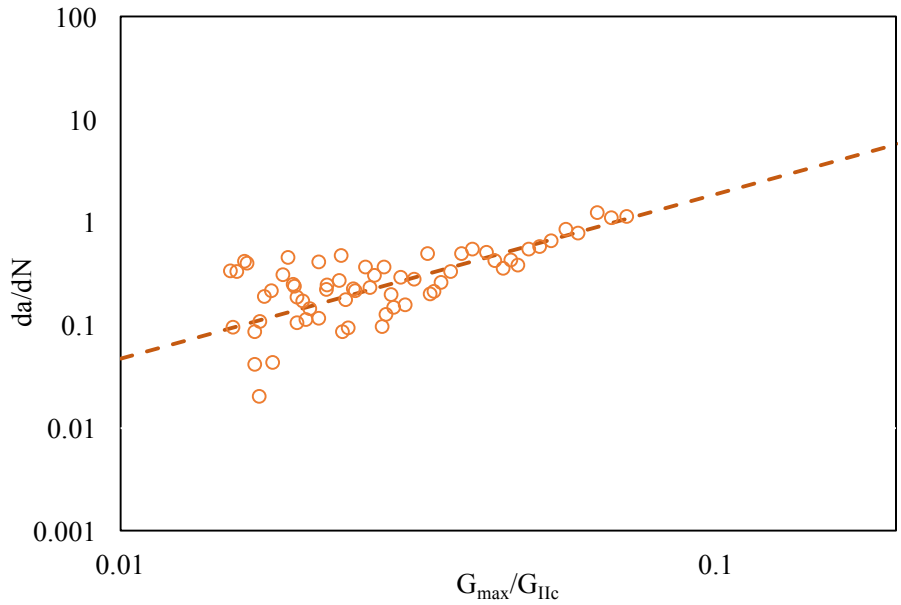

Figure 21 - Mode II component for mixed mode test (φ=45°)

Table 6 shows the results of the Paris law parameters obtained for the mixed mode tests with a load level of 60% and a load ratio of 10%.

Table 6 - Paris law constants of the mixed mode specimens tested (φ=45°)

Mode I component			Mode II component		
Intercept, c	Slope, m	G_{th}	Intercept, c	Slope, m	G_{th}
0.8 ± 0.11	1.86 ± 0.08	0.21 ± 0.04	75.8 ± 1.33	1.53 ± 0.07	0.01 ± 0.001

According to the results given in Table 6, the slope for mode II component has a smaller value which states that the crack growth rate in mode II is lower than mode I, even when the phase angle is 45^{o} for the mixed mode conditions.

Figure 22 shows the slope envelope of the Paris law for the load level of 60% and the ratio of 10%. Observing the envelope of m (slope of the Paris law curve), it can be concluded that the crack propagation rate verified in pure mode II is lower than in pure mode I.

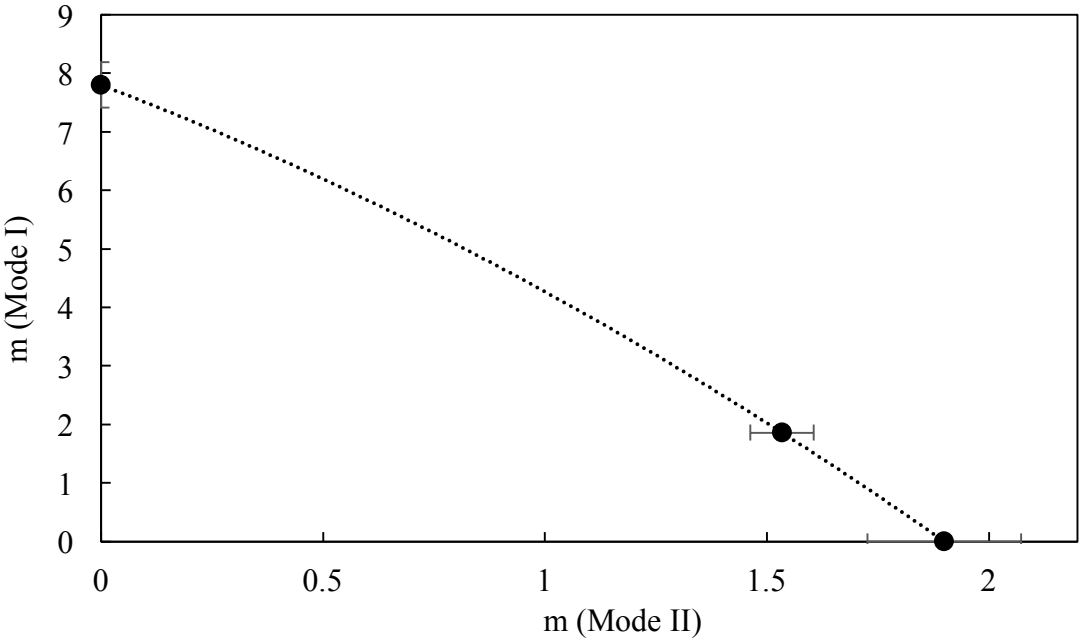

Figure 22 - Paris law slope envelope

5. Conclusions

The static and fatigue behavior of a structural epoxy-based adhesive was studied under pure and mixed loading modes. Based on the static results, the fracture envelope of the adhesive was experimentally obtained. The adhesive was also characterized in terms of fatigue crack propagation using the Paris law method. Based on the results, the m envelope was obtained as a function of different mode mixities. Different loading conditions were considered to study the effects of load level and R ratio on the fatigue behavior of the adhesive. It was observed that the use of higher load (amplitude) leads to a faster crack propagation and consequently a shorter life. Result showed that the effect of load level on fatigue crack propagation is more pronounced for lower *R*-ratios. It was also found that the G_{th} can be considered as constant for different mode I loading conditions. However, it was also observed that G_{th} is a function of the mode mixity.

Based on the results, it can be stated that by increasing the load level at similar R ratio, the difference between the G_{min}/G_{max} and R^2 increases. On the other hand, by keeping the load level constant and increasing the R ratio again it was found that the difference

between the G_{min}/G_{max} and R^2 decreases. Accordingly, when the crack faces are closer during the unloading process, the difference between the R^2 and G_{min}/G_{max} is higher. Some possible reasons for this behavior are the crack closure phenomenon, difficulty in measuring the G_{min} and also the employed data reduction approach.

References

1. LFM. Da Silva, A. Öchsner, R.D. Adams, Handbook of adhesion technology, Springer Science & Business Media, Berlin Heidelberg, 2011.
2. H. Khoramishad, AD. Crocombe, KB. Katnam, Predicting fatigue damage in adhesively bonded joints using a cohesive zone model. International Journal of Fatigue, 2010, **32**(7): p. 1146-1158.
3. H. Khoramishad, AD. Crocombe, KB. Katnam, A generalised damage model for constant amplitude fatigue loading of adhesively bonded joints, International Journal of Adhesion, 2010. **30**(6): p. 513-521.
4. L. Kawashita, MI. Jones, RS. Trask, SR. Hallet, MR. Wisnom, Static and fatigue delamination from discontinuous plies–experimental and numerical investigations. in Proceedings of the international conference on composite materials–ICCM, 27 - 31 July 2009, Edinburgh, United Kingdom.
5. M. Hojo, K. Tanaka, CG. Gustafson, R. Hayashi, Effect of stress ratio on near-threshold propagation of delimination fatigue cracks in unidirectional CFRP, Journal Composites Science Techonology, 1987, **29**(4) p.273-292.
6. C. Rans, R. Alderliesten, R. Benedictus, Misinterpreting the results: How similitude can improve our understanding of fatigue delamination growth. Journal Composites Science Techonology, 2011, **71**(2): p. 230-238.
7. R. Marissen, Fatigue crack growth in ARALL*:* A hybrid aluminium-aramid composite material: Crack growth mechanisms and quantitative predictions of the crack growth rates. Faculty of Aerospace Engineering, Report LR-574, 1988.
8. M. Hojo, T. Ando, M. Tanaka, T. Adanchi, S. Ochiai, Y. Endo, Modes I and II interlaminar fracture toughness and fatigue delamination of CF/epoxy laminates with self-same epoxy interleaf, International Journal of Fatigue 2006, **28**(10): p. 1154-1165.
9. D. Samborsky, A. Sears, J. Mandell, P. Agastra, Mixed mode static and fatigue crack growth in wind blade paste adhesives, in 52nd AIAA/ASME/ASCE/AHS/ASC Structures, Structural Dynamics and Materials Conference 19th AIAA/ASME/AHS Adaptive Structures Conference 13t, Denver,Colo 2011.
10. S. Azari, M. Papini, JA. Achroeder, JK. Spelt, The effect of mode ratio and bond interface on the fatigue behavior of a highly-toughened epoxy, Journal Engineering Fracture Mechanics, 2010, **77**(3): p. 395-414.
11. A. Pirondi, F. Moroni, An investigation of fatigue failure prediction of adhesively bonded metal/metal joints. International Journal of Adhesion, 2009, **29**(8): p. 796-805.
12. S. Razavi, MR. Ayatollahi, M. Samari, LFM. Da Silva, Effect of interface non-flatness on the fatigue behavior of adhesively bonded single lap joints.

Proceedings of the Institution of Mechanical Engineers, Part L: Journal of Materials: Design and Applications, 2017: p. 1464420717739551.
13. A. Pereira, PNB. Reis, JAM. Ferreira, Effect of the mean stress on the fatigue behavior of single lap joints. The Journal of Adhesion, 2017, **93**(6): p. 504-513.
14. M. Costa, G. Viana, LFM. Da Silva, RDSG. Campilho, Environmental effect on the fatigue degradation of adhesive joints: a review. The Journal of Adhesion, 2017. **93**(1-2): p. 127-146.
15. S. De Barros, PP. Kenedi, SM. Ferreira, S. Budhe, AJ. Bernardino, LFG. Souza, Influence of mechanical surface treatment on fatigue life of bonded joints. The Journal of Adhesion, 2017, **93**(8): p. 599-612.
16. ASTM, Annual Book of ASTM Standards, Standard test method for fracture strength in cleavage of adhesives in bonded metal joints, 1999, **15**: p. 212-218.
17. M. Costa, R. Carbas, E. Marques, G. Viana, LFM. Da Silva, An apparatus for mixed-mode fracture characterization of adhesive joints. Journal Theoretical Applied Fracture Mechanics, 2017, **91**: p. 94-102.
18. FJP. Chaves, LFM. Da Silva, M. De Moura, DA. Dillard, VHC. Esteves, Fracture mechanics tests in adhesively bonded joints: a literature review. The Journal of Adhesion, 2014, **90**(12): p. 955-992.
19. M. De Moura, RDSG. Campilho, JPM. Gon;alves, Pure mode II fracture characterization of composite bonded joints.International Journal of Solids, 2009, **46**(6): p. 1589-1595.
20. FJP. Chaves, LFM. Da Silva, M. De Moura, DA. Dillard, JO. Fonseca, Apparatus and method for characterization of bonded joints mixed-mode I ž II fracture, Universidade do Porto, submitted patent number: 20131000070010. 2013.
21. WS. Chan, AS. Wang, Free-edge delamination characteristics in S2/CE9000 glass/epoxy laminates under static and fatigue loads, in Composite Materials: Fatigue and Fracture, Second Volume, 1989, ASTM International.
22. G. Allegri, MI. Jones, MR. Wisnom, SR. Hallet, A new semi-empirical model for stress ratio effect on mode II fatigue delamination growth. Journal Composites Part A: Applied Science Manufacturing, 2011, **42**(7): p. 733-740.
23. RL. Ramkumar, JD. Whitcomb, Characterization of mode I and mixed-mode delamination growth in T300/5208 graphite/epoxy, in Delamination and debonding of materials, 1985, ASTM International.
24. DJ. Wilkins,JR. Eisenmann, RA. Camin, Ws. Margolis, RA. Benson, Characterizing delamination growth in graphite-epoxy, in Damage in Composite Materials: Basic Mechanisms, Accumulation, Tolerance, and Characterization. 1982, ASTM International.
25. DA. Jablonski, Fatigue crack growth in structural adhesives, The Journal of Adhesion, 1980, **11**(2): p. 125-143.